UNIVERSIDAD TÉCNICA FEDERICO SANTA MARÍA
DEPARTAMENTO DE FÍSICA

Cometary Water Delivery: N-body simulations of Non-Gravitational Forces in Early Earth Hydration

Judytza Tapia H.

THESIS TO OBTAIN THE DEGREE OF MASTER IN PHYSICS

Tutor: Dr. Matthias Schreiber
Co-tutor: Dr. Jorge Cuadra

JULY-2026

CONSTANCIA DE VALIDACIÓN Y CONFIDENCIALIDAD DE MONOGRAFÍA A REPOSITORIO ACADÉMICO

1.- IDENTIFICACIÓN DEL TRABAJO ACADÉMICO

Tipo de monografía (marcar una opción): ☐ Memoria o trabajo de título X Tesis de Postgrado

Título del trabajo:

Cometary Water Delivery: N-body simulations of Non-Gravitational Forces in Early Earth Hydration____

Nombre del candidato(a):

Judytza Anahis Tapia Henríquez____

Carrera / Grado:

Magíster en Ciencias, Mención Física____

Campus: Casa Central_________________ **Departamento:** Física____

2.- VALIDACIÓN DEL PROFESOR GUÍA/DIRECTOR DE TESIS

Yo, ______________________________Matthias Schreiber__________________________________, en mi calidad de profesor(a) guía/director(a) del trabajo académico mencionado anteriormente **DEJO CONSTANCIA** que:

- He revisado esta versión del documento y corresponde a la versión final aprobada del trabajo.
- El trabajo cumple con los requisitos académicos y de formato establecidos por la institución.

3.- EVALUACIÓN DE CONFIDENCIALIDAD POR PROPIEDAD INDUSTRIAL (marcar una opción)

X El trabajo **NO contiene** información que amerite confidencialidad y puede ser publicado de inmediato en repositorio con acceso abierto.

☐ El trabajo **CONTIENE** información con potenciales implicancias de propiedad industrial o intelectual y requiere un periodo de confidencialidad (**embargo**) por **(marcar una opción)**:

☐ 6 meses ☐ 12 meses ☐ 2 años ☐ 3 años ☐ 5 años ☐ 10 años

Fundamentación de la necesidad de confidencialidad (obligatorio si se solicita embargo):

4.- FIRMAS

Profesor(a) guía o director(a) de memoria o tesis:

Fecha: __________10.8.2026_______________ **Firma:** _____________________________________

Estudiante o Candidato(a):

Fecha: _03/08/2026_______________ **Firma:** ____

Este formulario debe ser insertado como página 2 de la memoria o tesis, completado y firmado por estudiante y profesor(a) antes de la entrega en portal PRISMA de Biblioteca USM.

Table of Contents

We saw the mirage in the desert but we couldn't grasp it
Praying that we'll remain in this desert till the end
Praying that this isn't truly our reality
In the end, we reached the mirage and it became our reality
The desert we feared was filled with our blood, sweat, and tears, and became an ocean

---

BTS, *Sea*

Chapter 1

Introduction

1.1 Solar System Formation

Approximately 4.57 billion years ago, the Solar System formed from the gravitational collapse of a dense region within a molecular cloud composed primarily of gas and dust. These clouds consist mostly of hydrogen but approximately one percent of their mass is found in the form of small dust grains. If the mass of a molecular cloud exceeds the critical Jeans-mass, it collapses and fragments. As the cloud contracted under its own gravity, most of the material accumulated at its center, giving rise to a proto star that would eventually become the Sun.

The Sun is thought to have formed within a stellar cluster containing between 2,000 and 10,000 stars, following the gravitational collapse of a molecular cloud. As the cloud contracted, conservation of angular momentum caused its rotation rate to increase, preventing all of the material from accreting directly onto the forming Sun. Instead, the remaining gas and dust settled into a flattened, rotating structure around the young star, known as the proto planetary disk (Pfalzner et al., 2015).

Proto planetary disks typically contain between 0.2% and 20% of the mass of their host star and have lifetimes of approximately 2–3 million years. Within these environments, microscopic dust particles underwent repeated collisions. When these collisions occurred at sufficiently low relative velocities, the particles could stick together through electrostatic and adhesive forces, forming progressively larger aggregates. From the disk, the first solids to form in the inner disk are refractory minerals known as CAIs (Calcium-Aluminum-rich Inclusions). They can be found inside chondritic meteorites. About 0.5 million years later, some dust grains start to grow from collisions, first forming porous aggregates and later pebbles (from mm to cm).

Over time, these aggregates grew from micron-sized grains to pebbles and, eventually, to kilometer-sized bodies known as planetesimals. Those pebbles start to concentrate in the high pressure regions by streaming instability. These concentrations gravitationally collapse and start to form the first planetesimals, from 100 to 1000 km of diameter. Once planetesimals formed, gravity became an increasingly important factor, enhancing further growth through collisions and accretion.

Continued accumulation of material produced larger planetary embryos, whose subsequent interactions and mergers ultimately led to the formation of the planets of the Solar System. On the first 5-10 million years, Jupiter and Saturn start to grow from the pebble accretion. First, they form a core of $\sim$10 earth masses in less than a million years, and subsequently they accumulate gasses in the disk until they reach their actual masses. Uranus and Neptune grow at a slower pace because their regions has less pebbles, and attract only a few Earth masses of gas, becoming "Ice Giants". The gas disk dissipates after 2-10 million years, stopping the giants growth.

The composition of the bodies formed within the proto planetary disk was strongly influenced by its thermal structure. Temperatures decreased with increasing distance from the young Sun, resulting in different materials condensing at different locations within the disk. While only high-temperature materials could remain solid in the warmer inner regions, volatile compounds such as water could condense into ice in the colder outer regions. The transition between these regimes is commonly referred to as the snow line, which marks the distance from the Sun beyond which water ice could exist in solid form. Consequently, planetesimals formed beyond the snow line incorporated significantly larger amounts of water and other volatiles than those formed closer to the Sun, establishing the outer Solar System as an important reservoir of icy bodies.

Among the icy bodies that formed beyond the snow line, comets are of particular interest due to their high volatile content and their relatively pristine nature, preserving material from the early stages of Solar System formation. Together with other populations of small bodies in the outer Solar System, they represent important reservoirs of water and other volatile compounds.

After the gas disk dissipated (around 2–10 million years), the giant planets kept interacting gravitationally with the remaining planetesimal disk. Jupiter migrated inward, while Saturn, Uranus and Neptune migrated outward. When Jupiter and Saturn crossed their orbital resonance, a violent instability was triggered, and planetesimals were dispersed all over the system. These planetesimals collided with each other, starting to form proto planets. Mars formed around 2–10 million years, and its small size was due to Jupiter cutting off its material supply. Earth took between 38 and 120 million years to reach its current size, with volatile elements like water delivered during its final growth stages. In contrast, Earth formed in the warmer inner regions of the proto planetary disk, where water ice could not readily condense. This apparent discrepancy raises a fundamental question: if our planet formed in a relatively dry environment, how did it acquire the vast amounts of water observed today in its oceans, atmosphere, and interior? The instability also triggered the Late Heavy Bombardment (LHB), a period around 3.8–4.1 billion years ago when the inner planets suffered intense impacts, dispersing objects from the asteroid belt and the Kuiper

Belt. For the first 6 Gyr, the Sun will remain on the main sequence, where the inner planets have a 98–99% survival probability without collisions.

Even if the LHB is often displayed as a catastrophe that threatened the recently formed planets, it was also an important episode for their enrichment. The gravitational instability that dispersed objects from the Asteroid Belt and Kuiper Belt didn't only generate a lethal projectiles rain, it also transported to the Solar System elements that would make the Earth habitable. It is considered that the most important element to sustain life is water. Nevertheless, before this period Earth was too hot to have it. It was believed that the only way we have this vital element nowadays it's because of external precedences.

1.2 Origin of Water on Earth

From the traditional model Oort, 1950; Fernández, 1978, the Oort cloud is formed form the planetesimals dispersed from Uranus and Neptune. They produce small energy changes letting comets be trapped in bonded orbits ($\sim 10^4$ AU). However, Fernández 1997 points outs that Jupiter and Saturn also control the dynamic evolution of the Oort cloud comets. Many researches question about the water delivery from these comets, trans-Neptunian objects and water-rich meteorites.

The most important parameter considered is the D/H (Deuterium/Hydrogen) ratio. It is fundamentally measured because it works as chemist "fingerprint", and it helps to measure the Solar System origin. Normal Hydrogen posses only one proton in its nucleus, while deuterium posses a proton and a neutron. In water, it measures how many molecules of "heavy water" (HDO) are in comparison to normal water (H_2O) (Lis et al. 2019).

The origin of Earth's water has been extensively debated, with several mechanisms proposed to explain how our planet acquired its volatile inventory. These mechanisms can be broadly classified into two categories: external delivery by bodies formed beyond the snow line, and internal production through planetary processes. Morbidelli et al. 2000 provides a comprehensive framework for evaluating the external delivery mechanisms, which include the following pathways:

1.2.1 Planetary Embryos

Numerical simulations by Chambers and Wetherill 1998 and Morbidelli et al. 2000 model the formation of the rocky planets from a disk of planetary embryos distributed between 0.5 and 4 AU. Embryos originating beyond 2.5 AU—the region of carbonaceous asteroids—are water-rich, with D/H ratios similar to that of Earth's oceans. In 11 simulations, Earth accreted between 1 and 3 primitive embryos, representing 10–25% of its final mass. This mechanism suggests that a significant fraction of Earth's water could have been delivered during its final accretion stages.

1.2.2 Asteroids

The same simulations were also run with asteroids treated as test particles (massless). Using the collision probability code of Farinella and Davis 1992, it was found that only 0.13% of the initial asteroidal mass collides with Earth. For this to contribute significantly, the asteroid belt would need to have had an initial mass of $\sim M_{\oplus}$—a scenario that is physically plausible. However, this delivery would need to have occurred when Earth had less than 60% of its final mass; otherwise, most of the water would have been lost in later impacts.

Two additional mechanisms have been proposed to enhance asteroidal delivery:

Secular Resonance Sweep Ward et al., 1976; Gomes, 1997: Secular resonances occur when the precession frequency of an asteroid's perihelion matches that of a planet. These resonances gradually increase the asteroid's eccentricity until its orbit crosses that of a planet. If Jupiter and Saturn migrate radially, or if the proto planetary nebula dissipates, these resonances can sweep across the asteroid belt. For asteroids at 2.5 AU, this mechanism yields a collision probability with Earth of $\sim 10^{-3}$; for asteroids farther out, the probability drops to $\sim 10^{-6}$. Thus, without the contribution of massive embryos, the amount of water delivered by the outer asteroid belt is negligible.

Gas Drag Franklin and Lecar, 2000: When a small asteroid (5–10 km in diameter) acquires an eccentricity greater than 0.2–0.3 through resonances, friction with the nebular gas reduces its semi major axis, causing it to spiral inward. According to these models, 97.8% of small asteroids (5–10 km) from the outer belt end up with semi major axes below 2 AU. For larger asteroids (10–20 km), 71% reach the inner region, where Earth's collision probability reaches 5%. However, this mechanism has two major limitations: (i) it must operate at an early stage, when Earth was still small, so that later impacts would remove most of the delivered water; and (ii) these models fail to reproduce the observed inclinations of surviving asteroids Nagasawa et al., 2000.

1.2.3 Comets

Morbidelli et al. 2000 simulated 6000 test particles with semi major axes between 4.5 and 9 AU (the Jupiter-Saturn region), initially with zero eccentricity and inclination, using the integrator *swift-mvs3* Levison and Duncan, 1994. The collision probability with Earth was found to be $1 \sim 3 \times 10^{-6}$, and 90% of the particles escaped the system within 2 million years. According to planetary formation models Pollack et al., 1996; Hahn and Malhotra, 1999, the initial mass of the cometary reservoir was between 50 and 100 $M_{\oplus}$. If comets were 100% ice, the total water mass delivered would be 10-60% of Earth's current ocean mass. However, accounting for water loss during impacts, the authors estimated a more realistic contribution of 2-20%. For comets originating beyond Uranus, the delivery is about $\sim 10\%$ Levison et al., 2000. By the year 2000, none of these external delivery models provided a fully satisfactory explanation, largely because they neglected an important factor: non-gravitational forces.

1.2.4 Earth's Mantle: An Internal Source

A recent experiment by Miozzi et al. 2025 suggests an alternative, internal mechanism for the origin of Earth's water. The experiment simulates the extreme pressure and temperature conditions inside young planets, specifically sub-Neptunes (planets with sizes between Earth and Neptune). However, the results are directly applicable to primordial Earth and other rocky planets that possessed a hydrogen-rich primary atmosphere over a magma ocean.

The experiment demonstrates that when atmospheric hydrogen reacts with molten magma rich in iron oxide (FeO), it produces large amounts of water (H_2O) and metallic iron (Fe):

$\mathrm{FeO} + \mathrm{H_2} \longrightarrow \mathrm{Fe} + \mathrm{H_2O}$

If this process were efficient, Earth could have acquired water equivalent to several oceans in its first million years. However, the experiment has limitations for the terrestrial case: it used pressures up to 60 GPa and temperatures of 4000 K, conditions that exceed those of the standard Earth's upper mantle ($\sim$24 GPa), which likely only occurred after giant impacts, such as the one that formed the Moon. These extreme pressures were specifically chosen to simulate sub-Neptunes and identify the 45 GPa threshold for complete miscibility. Below this pressure, the water produced remains as a separate "free-flowing phase" (forming bubbles or cavities), while above 45 GPa, the system becomes completely miscible in a single supercritical phase.

1.2.5 Nebular Water Steam Adsorption

An alternative early-Earth model was proposed by Drake 2005, who considered the adsorption of water vapor from the proto planetary nebula onto dust grains. In this scenario, the nebula contained approximately 2 $M_\oplus$ of water vapor—more than the total water mass of all the rocky planets combined. Using the physisorption model of Stimpfl et al., 2004, they calculated the amount of water that could have been adsorbed by the grains as a function of temperature:

- At 1000 K, only 0.25% of Earth's ocean mass could be adsorbed.
- At 700 K, 1%
- At 500 K, 3%

These percentages represent the fraction of Earth's current ocean mass that could have been delivered through this mechanism, assuming spherical grains. If the surface area of the grains is increased by a factor of 100 (a more optimistic scenario), the adsorbed water fractions rise to:

- At 1000 K: 0.25 of Earth's ocean mass
- At 700 K: 1 ocean mass
- At 500 K: 3 ocean masses

The model also considers chemisorption, where H_2O molecules bond with $Si-O-H$ clusters through hydrogen bridges and stronger bonds. If this process persists at higher temperatures, the adsorbed water could be better retained during planetary collisions. However, a major contradiction of this model is that the predicted D/H ratio of the adsorbed water does not match the D/H ratio of Earth's oceans.

1.3 The D/H Ratio Problem

For the theory that water has come from comets, it was measured the D/H ratio of comets, having 200% to 300% more times than the water of Earth, and it was assumed that comet can't be the main source of water on Earth (Eberhardt et al. 1995). Lécuyer et al. 2017 made 41 experiments simulating the sublimation of ice in space. They found that this process changed the D/H measured, but in a small scale that doesn't justify the difference between comets and Earth's D/H.

The belief that most comets have a higher D/H ratio than Earth was challenged by Lis et al. 2019, who propose that the D/H ratio of many comets is misinterpreted due to a failure to consider their hyperactivity.

They observed comet 46P/Wirtanen with a value identical to that of Earth's ocean, placing it in the category of a hyperactive comet. These comets produce more water vapor than their nuclear surface allows due to the ejection and sublimation of ice grains. Comets with an active phase tend to show D/H values consistent with Earth's water, while measurements of low-activity comets could be biased. The vapor could be enriched in deuterium through fractionation processes in non-stationary sublimation regimes, meaning it appears to contain more deuterium than it actually does.

This was observed in comet C/2014 Q2 where millimeter-scale measurements (which detect water from ice grains) showed a terrestrial value, while infrared observations (which detect vapor from the nucleus) measured a much higher D/H.

Although comets were historically dismissed as the source of Earth's water because initial measurements of objects like 1P/Halley showed deuterium levels far exceeding those of our oceans, recent studies have transformed this paradigm by revealing genuine diversity in the D/H ratio of the cometary population. Additionally, newer researches on comets such as 12P/Pons–Brooks, 46P/Wirtanen, and 103P/Hartley 2 has documented values consistent with those found in Earth's ocean water (Cordiner et al. 2025).

1.4 Non-Gravitational Forces (NGF)

In 1819 the astronomer Johann Franz Encke discovered the comet with the shortest orbital period (3.3 years). Nevertheless, the comet's period was smaller than predicted with purely gravitational forces. This comet, 2P/Encke, was decreasing its orbital period by 2.5 hours by revolution. This was also found in the comets 3D/Biela and 16P/Brooks. This was studied 100 years later when it was more known about the comet's ice nucleus. Whipple proposed in 1950 there's a non gravitational force acting like a jet from the non-isotropic sublimation of gases that get expelled from the comet.

First, there were considered three components of the non-gravitational force effect: J_x,J_t,J_n, which are the radial, transverse and normal non gravitational components. In 1973 Marsden et al. described those effects as $J_x = A_1 g(r)$, $J_t = A_2 g(r)$, $J_n = 0$, where:

$$g(r) = \alpha \left(\frac{r}{r_o}\right)^{-m} \left[1 + \left(\frac{r}{r_o}\right)^{n}\right]^{-k} \tag{1.1}$$

Here $\alpha = 0.1113$, $g(1) = 1$, $m = 2.15$, $n = 5.093$, $k = 4.6142$ and $r_o = 2.808$AU. This is a fit from the Delsemme and Miller 1971 curve for sublimation rate of snow.

Including non-gravitational forces is essential for modeling the long-term orbital evolution of comets. While gravitational forces act through well-defined planetary interactions, NGFs arise from a recoil or propulsive force produced by the sublimation of volatile ice in the comet's nucleus (Whipple 1950; Marsden et al. 1973). These forces are systematic and cumulative, acting principally closer to the perihelion, where solar warming is at its maximum for the sublimation rate (Sekanina 2021).

The final model is from Królikowska 2004 adding the A_3 parameter:

$$F_i = A_i g(r) \tag{1.2}$$

$$i = 1, 2, 3 \tag{1.3}$$

This parametrization, using the three components—radial A_1, transverse A_2, and later added, A_3, allows us to model the orbital evolution of a comet over several orbits (Marsden et al. 1973; Królikowska 2001). Additionally, they must be determined from astrometric observations for each comet individually, and they can change throughout time as the nucleus evolves (Sekanina 1972).

Nevertheless, the amount of these parameters is influenced by the family type of the comets. An easier way to categorize comets by family type is the Tisserand Parameter.

1.5 Tisserand Parameter

The Tisserand parameter was defined by the astronomer François Félix Tisserand and is used in the three-body problem. In this context, one considers a large object, μ_1 (in this case, the Sun), a planet orbiting that object, μ_2, and a smaller object, μ_3, whose mass is infinitesimal compared to μ_1 and μ_2.

$$T = \frac{a_2}{a_3} + 2 \cdot \sqrt{\frac{a_3}{a_2}(1 - e_3^2)} \cos(i_3) \tag{1.4}$$

Where a_2 is the major semi axis of the planet (for this classification Jupiter), and a_3, e_3, i_3 are the orbital parameters of the comet.

This parameter provides us with a clearer classification of each comet.

Comets with $T_J > 3$ are the comets closest to the Sun, with orbits smaller than Jupiter's and lower eccentricities. These comets will be called 'Asteroid Belt Family Comets' in the following analysis. Subsequently, comets with $2 < T_J < 3$ are considered 'Jupiter Family Comets', whose orbits are the closest to Jupiter's. Finally, comets with $T_J < 2$ are long-period comets with the highest eccentricities, which we call 'Oort Family Comets'.

Chapter 2

Research Objectives

The principal objective of this thesis is to quantify the effect of NGF on the probability that of a comet has an encounter with the Earth. Specifically:

1. How the inclusion of NGF affects the total number of encounters with the Earth? We compared simulations with and without Marsden 1973 model to determine if these encounters increases, decreases, or remain unchanged.

2. Which component of the NGF is the most significant? Marsden 1973 model includes radial, transversal and normal components. We examine which one of these increases the encounter probability.

3. How different is the NGF effect depending of the comet family? Comets are traditionally classified by their Tisserand parameter. We examine if the NGF differs between populations.

4. What is the role of planetary perturbations on these encounters? We compare simulations with and without solar system planets to discern between the NGF effect and planets gravitational effect.

5. Does the addition of NGF modify the encounter probability calculated previously? How does this affect current theories of water arrival on Earth?

Chapter 3

Methods

Our objective is to do a simulation of a thousand comets for 100,000 years, considering the interaction of non-gravitational forces and planetary interaction.

The main code that was used is `REBOUND`.
"`REBOUND` is an N-body integrator, i.e. a software package that can integrate the motion of particles under the influence of gravity. The particles can represent stars, planets, moons, ring or dust particles. `REBOUND` is very flexible and can be customized to accurately and efficiently solve many problems in astrophysics."

`REBOUND` refers as Orbital elements as:
`a` : Semi-major axis [AU]
`e` : Eccentricity
`inc` : Inclination (Radians) $[0,\pi]$
`Omega` : Ascending node (Ω) $[-\pi,\pi]$
`omega` : Argument of Peri-apsis (ω) (Radians) $[-\pi,\pi]$
`f` : True Anomaly (f) (Radians) $[-\pi,\pi]$
This code can be run on *Python*, with:

```
import rebound
import numpy as np
sim = rebound.Simulation()
```

To carry out a representative simulation, we modeled 1,000 comets classified between three dynamic families. They are not fully representative of the amount of comets in the Solar System, but were used for testing purposes.

- **Jupiter Family (50%):** This population represents the principal source of short-period comets in the inner Solar System. Their higher proportion (50%) reflects the efficiency of Jupiter's gravitational perturbations in capturing objects from the Kuiper Belt and scattering them into the inner Solar System Levison and Duncan, 1994. These comets typically have orbits with semi major axes between 2.5 and 6.0 AU, moderate to high eccentricities (0.4–0.85), and low inclinations (0°–30°), consistent with the observed orbital distribution of Jupiter-family comets Levison et al., 2000. The bifurcation in eccentricity (60% with $e < 0.7$, 40% with $e > 0.7$) accounts for the diversity of dynamical histories among these objects, including those that have undergone multiple close encounters with Jupiter.

- **Asteroid Belt Family (30%):** These are objects with smaller orbits that are less affected by Jupiter's perturbations, and with generally lower eccentricities. Based on Bottke et al. 2002, this population is formed from main-belt asteroids that undergo the Yarkovsky effect,a thermal radiation force that causes a slow drift in semi major axis, eventually bringing them into resonances that pump their eccentricities to Earth-crossing values. The Yarkovsky effect is significant for asteroids smaller than 30–40 km in diameter, which is the size range we modeled here Vokrouhlický et al., 2015. Their semi major axes (2.0–3.5 AU), eccentricities (0.2–0.6), and inclinations (0°–20°) are chosen to represent the typical orbits of objects that can evolve into near-Earth space via the ν_6 secular resonance and the 3:1 mean-motion resonance with Jupiter Bottke et al., 2002. The condition $a(1 - e) < 0.5$ ensures that the comet crosses Earth's orbit, making encounters possible. As our simulation has only 100,000 years, comets with a higher perihelion have less chances of modifying their orbit in such a short time, specially without NGF. This kind of condition was also used by Bottke et al. 2002 for Near Earth Objects (NEOs).

- **Oort Cloud Family (20%):** These are comets with orbits beyond Jupiter's semi major axis and periods exceeding 200 years. We include Halley-type comets ($20 < P < 200$ years) in this category, as they share similar dynamical characteristics Levison and Duncan, 1994. Their high eccentricities ($0.95 - 0.999$) facilitate interactions with the giant planets, although they spend most of their orbital period far from the Sun, in the outer Solar System or the Oort cloud. Their inclinations are uniformly distributed between 0° and 180° to reflect the isotropic nature of the Oort cloud population Dones et al., 2004. They represent the smallest fraction (20%) because of their extremely long return times and the low probability that they will be perturbed into the inner Solar System during the 100,000-year integration time Dones et al., 2004.

The values used for NGF aren't universal constants but a synthetic model selected to represent the observed variability of a real population. Additionally, it was considered a dynamic maturity respective to their planet family. Oort Family Comets haven't orbited many times around the sun such as Asteroid Belts Comets, thus their A_1 and A_2 parameters are higher, with also a higher dispertion Królikowska 2004. This is explained as their NGF decays as the comet loses their ice layers (Sekanina 1988). This is why Asteroid Belt and Jupiter comets have lower A_1 and A_2. Their sign can be positive or negative depending of their rotation axis.

The parameter A_3 requires a very specific configuration, as it's rare it's configured for only 10% of comets to simplify our simulations. The normal component A_3 of the non-gravitational acceleration is a direct consequence of the anisotropy in cometary nucleus out gassing. According to Sekanina 1981 and Marsden et al. 1973, the resultant force of the sublimation jets depends on the orientation of the comet's rotation pole with respect to its orbital plane. Mathematically, the A_3 component only acquires significant values when there is a component of the out gassing force vector projected outside the orbital plane. In synthetic populations, since the orientation of the rotation axis is a stochastic variable, most of the population exhibits pole orientations that result in A_3 values close to zero, or they are cases where the vector sum of the jets on the nucleus tends to cancel perpendicular to the orbital plane.

```
import random
import math

def generate_comet_jupiter_family():
    a = random.uniform(2.5, 6.0)
    if random.random() < 0.6:
        e = random.uniform(0.4, 0.7)
    else:
        e = random.uniform(0.7, 0.85)
    if a * (1 - e) < 0.2:
        e = 1 - 0.2 / a
    inc = math.radians(random.uniform(0, 30))
    Omega = random.uniform(0, 2*math.pi)
    omega = random.uniform(0, 2*math.pi)
    f = random.uniform(0, 2*math.pi)
    return a, e, inc, Omega, omega, f

def generate_comet_belt():
    a = random.uniform(2.0, 3.5)
    e = random.uniform(0.2, 0.6)
    if a * (1 - e) < 0.5:
        e = 1 - 0.5 / a
    inc = math.radians(random.uniform(0, 20))
```

```
    Omega = random.uniform(0, 2*math.pi)
    omega = random.uniform(0, 2*math.pi)
    f = random.uniform(0, 2*math.pi)
    return a, e, inc, Omega, omega, f

def generate_comet_oort():
    a = random.uniform(20.0, 100.0)
    e = random.uniform(0.95, 0.999)
    inc = math.radians(random.uniform(0, 180))
    Omega = random.uniform(0, 2*math.pi)
    omega = random.uniform(0, 2*math.pi)
    f = random.uniform(0, 2*math.pi)
    return a, e, inc, Omega, omega, f
```

And their parameters A_1, A_2 and A_3:

```
def generate_parameters_ng(population):
    if random.random() < 0.1:
        a3 = random.uniform(0.001, 0.05) * 1e-8 * random.choice([1, -1])
    else:
        a3 = 0.0
    if poblacion == 'jupiter':
        a1 = random.uniform(0.05, 1.5) * 1e-8
        a2 = random.uniform(0.01, 0.3) * 1e-8 * random.choice([1, -1])
    elif poblacion == 'belt':
        a1 = random.uniform(0.01, 0.8) * 1e-8
        a2 = random.uniform(0.005, 0.2) * 1e-8 * random.choice([1, -1])
    else:  # oort
        if random.random() < 0.7:
            a1 = random.uniform(0.1, 2.0) * 1e-8
        else:
            a1 = random.uniform(2.0, 8.0) * 1e-8
        a2 = random.uniform(0.01, 0.5) * 1e-8 * random.choice([1, -1])
    return a1, a2, a3
```

REBOUND offers a wide range of integrators depending of the type of simulation and the objective precision. In this study, we used ias15, whose variable timestep allows the integration to automatically adjust its temporal resolution according to the dynamical evolution of the system. This ensures high accuracy while reducing the number of unnecessary integration steps and, consequently, the computational cost.

It is crucial to add the Sun as the main object where the simulation revolves around. Subsequently, the planets are added. REBOUND allow us to add the name of the objects, and it connects with NASA Horizons System to add the object in a specific time. Nevertheless, for further simulations, the planets where added with their specific orbital elements, assuring us to always have the same results.

```
sim.integrator = "ias15"
sim.add("Sun")
sim.add("Earth")
```

The comets were added next:

```
with open('comets.txt', 'r') as f:
    encabezado = next(f).strip().split(',')
    for numero_cometas, linea in enumerate(f, 1):
        datos = list(map(float, linea.strip().split(',')))
        sim.add(m=0, a=datos[0], e=datos[1], inc=datos[2],
                    Omega=datos[3], omega=datos[4], f=datos[5])
sim.move_to_com()
fig= rebound.OrbitPlot(sim, unitlabel="[AU]")
ax = fig.fig.axes[0]
ax.set_xlim(-4, 4)
ax.set_ylim(-4,4)
fig.fig.tight_layout(rect=[0, 0, 1, 0.95])
```

Adding a thousand comets, our simulation looks like the following Orbit plot 3.1

As REBOUND only considers gravitational forces, the NGF were added manually with the function described by Chambers 2012:

```

def propulsion_force(sim,params):

    j=8
    k=0
    while j<sim.contents.N:
        A1,A2,A3=params[k]
        x = sim.contents.particles[j].x - sim.contents.particles[0].x
        y = sim.contents.particles[j].y - sim.contents.particles[0].y
        z = sim.contents.particles[j].z - sim.contents.particles[0].z
        vx = sim.contents.particles[j].vx - sim.contents.particles[0].vx
```

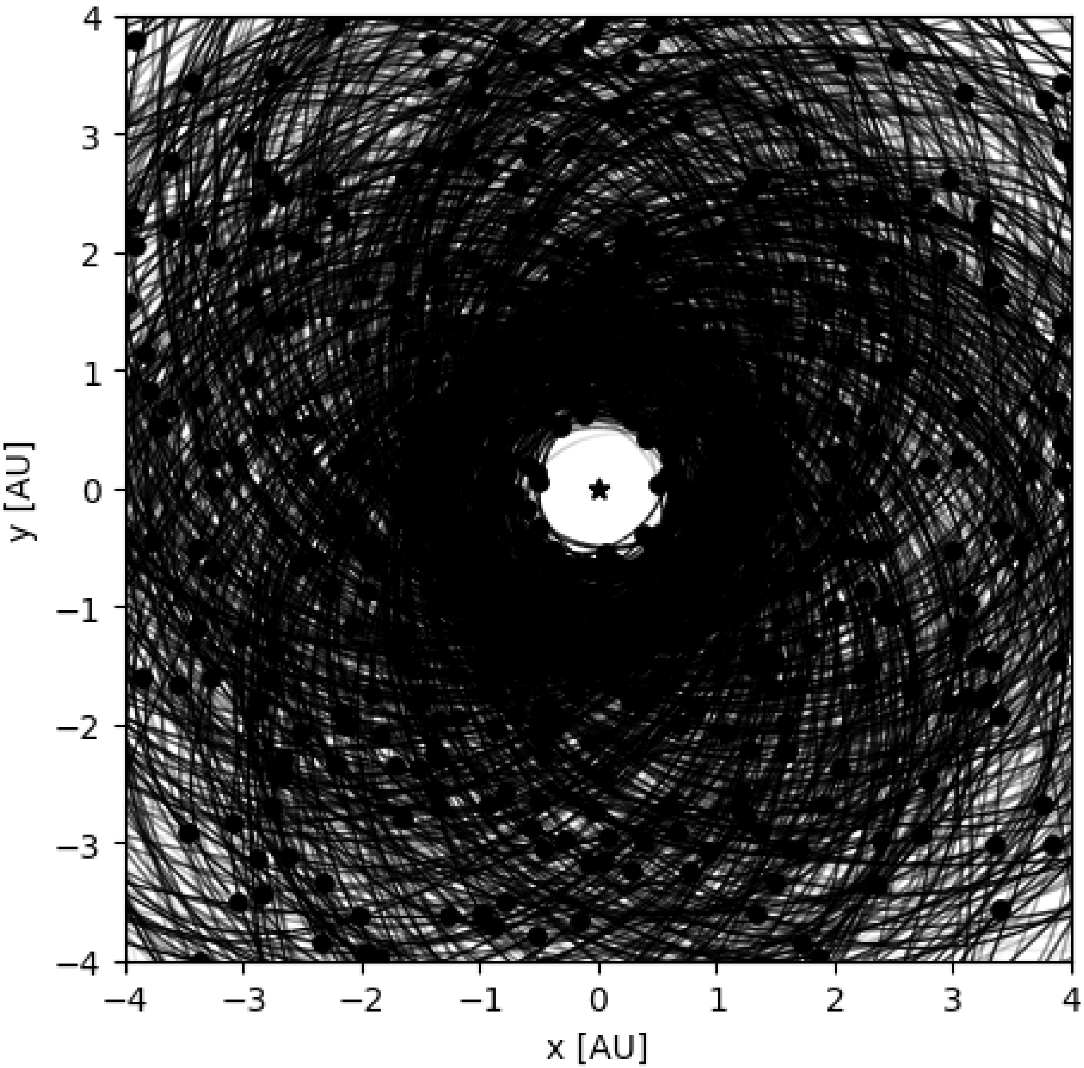

Figure 3.1: This plot displays the position of 1000 random comets around the Sun, in a 4 AU radius

```
        vy = sim.contents.particles[j].vy - sim.contents.particles[0].vy
        vz = sim.contents.particles[j].vz - sim.contents.particles[0].vz
        r2 = x*x + y*y + z*z
        r = np.sqrt(r2)
        if r2 < 88.0 or abs(A1) > 1e-7 or abs(A2) > 1e-7 or abs(A3) > 1e-7:
            rv = x*vx + y*vy + z*vz
            q = r* 0.3561253561253561
            g = 0.111262 * q**(-2.15) * (1.0 + q**5.093)**(-4.6142)
            tx = r2*vx - rv*x
            ty = r2*vy - rv*y
            tz = r2*vz - rv*z

            nx = y*vz - z*vy
            ny = z*vx - x*vz
            nz = x*vy - y*vx

            a1 = A1 * g / r
            a2 = A2 * g / np.sqrt(tx*tx + ty*ty + tz*tz)
            a3 = A3 * g / np.sqrt(nx*nx + ny*ny + nz*nz)

            sim.contents.particles[j].ax += (a1*x + a2*tx + a3*nx) * (365.25**2)
            sim.contents.particles[j].ay += (a1*y + a2*ty + a3*ny) * (365.25**2)
            sim.contents.particles[j].az += (a1*z + a2*tz + a3*nz) * (365.25**2)
        j+=1

def additional_forces(sim):
    propulsion_force(sim, params_a)

sim.additional_forces = additional_forces
```

Following, we consider a possible encounter as when the comet enters the zone of the Hill's radius. As Earth can be in any position around the zone, we consider all the area around the sun where the Earth can be, creating a "Hill's Ring", which is displayed in Plot 3.2 and Plot 3.3.

If we register directly every encounter with Earth would be computationally expensive and not efficient, as the impact probability is low. In exchange, considering every "possible encounter" as the "Hill's ring zone" will give us wider results, statistically significant without the necessity of simulate every encounter. Additionally, using direct physical collisions to determine the probability of impact in a numerical simulation carries the risk of introducing significant statistical bias due to the problem of "small-number statistics." Since physical collisions are stochastic and extremely rare events, relying solely on directly recorded impacts could lead to results that depend on the random trajectory of one or a few individual particles, which would not necessarily represent the overall behavior of the population Greenstreet et al. 2012. For this, we calculate the distance of

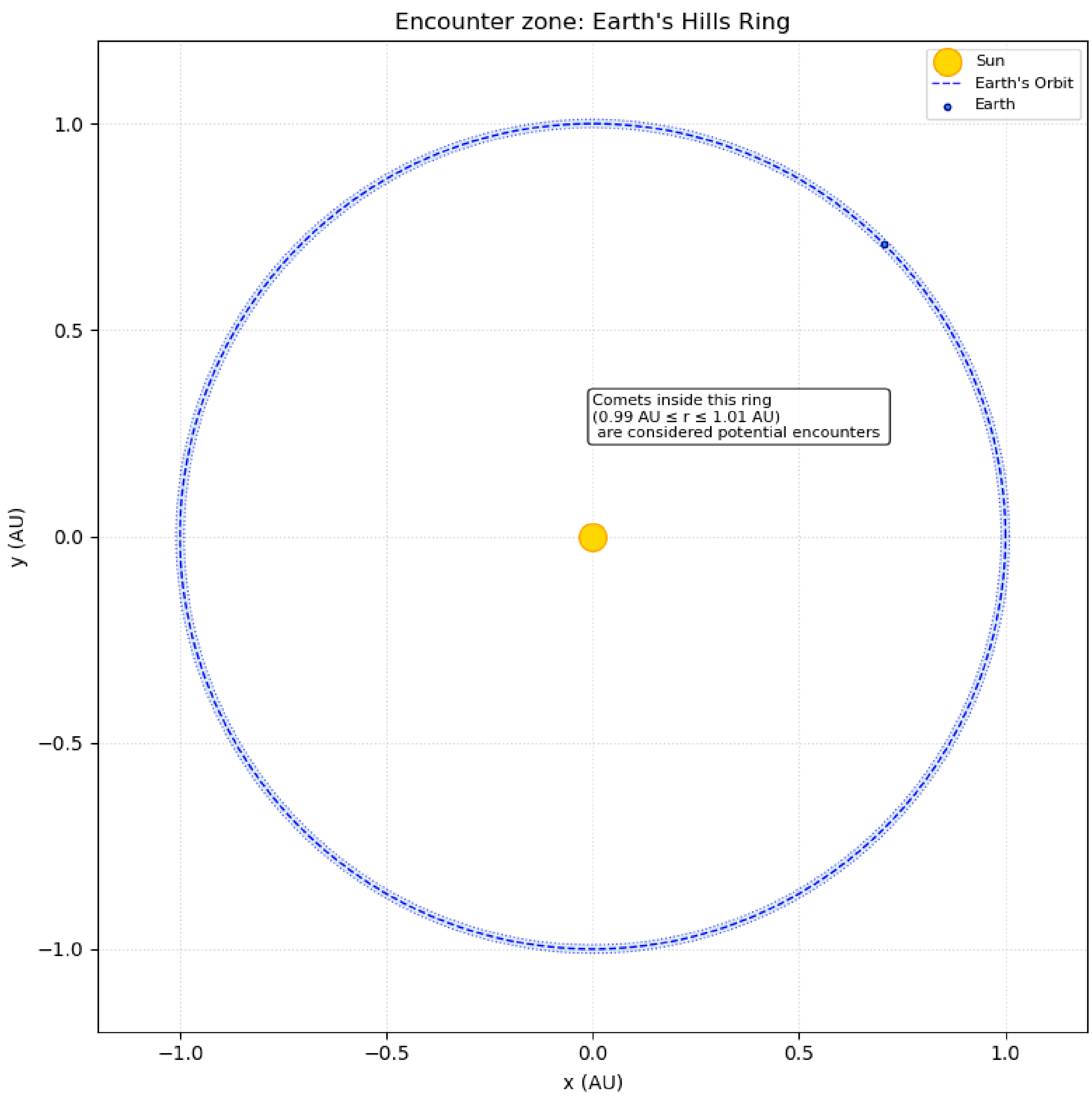

Figure 3.2: This plot displays the area of the Hill Radius all around the sun, forming a ring. This is the zone where we consider a possible encounter.

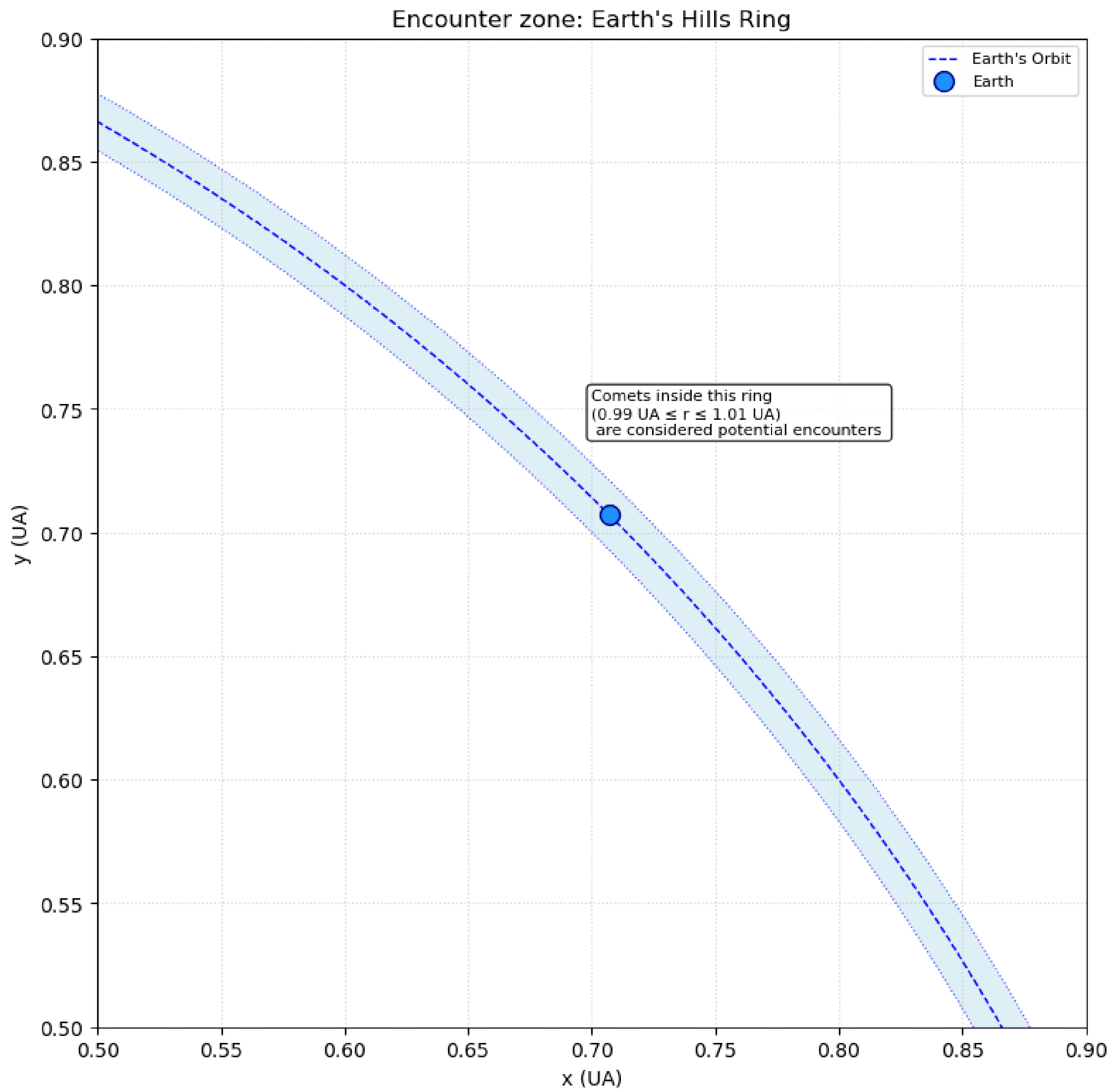

Figure 3.3: This plot is a zoomed version of 3.2, where we can see the planet Earth and the zone Hill's ring area around it.

the comet from the sun, and create a condition to save our encounter.

```
def distance(x1,y1,z1,x2,y2,z2):
    distance_earth=((x1-x2)**2+(y1-y2)**2)**(1/2)
    return distance_earth

#...
#inside our simulation
def heartbeat(sim):

    sun=sim.contents.particles[0]
    comet=sim.contents.particles[i]
    comet_distance=distance(sun.x,sun.y,sun.z,comet.x,comet.y,comet.z)

    if 0.99 < comet_distance < 1.01 and -0.01<comet.z< 0.01:
        print("Alert","Year: ", (sim.contents.t),"Cometa: ",i)
        encounters.append(i)
        sim.contents.remove(i)
    globalcounter+=1
```

Once we have an encounter, the comet is removed to fasten our simulation. Still, this function has a flaw. We can see the position of the comet before and after every timestep. If the distance the comet travels is longer than the Hill's radius, we could miss an encounter. Because of this, it was created a function to predict this. This function estimates the distance that the comet is going to travel on the next timestep, and if it's longer than the Hill's radius, predicts small steps where the comet is going to cross.

```
def predict_collision(sim, particle_idx, t):
    sun = sim.contents.particles[0]
    comet = sim.contents.particles[particle_idx]

    x,y,z=comet.x, comet.y, comet.z
    vx, vy, vz = comet.vx, comet.vy, comet.vz
    xx = vx * t
    yy = vy * t
    zz = vz * t
    current_dist = distance(sun.x, sun.y, sun.z, x, y, z)
    if not (0.5 < current_dist < 2):
        return False

    if 0.02 < abs(xx) or 0.02 < abs(yy) or 0.02 < abs(zz):

```

```
        if abs(xx) > abs(yy) and abs(xx) > abs(zz):
            steps = int(abs(xx) / 0.00001)
            step_size = t / steps
            for _ in range(steps):
                x += vx * step_size
                y += vy * step_size
                z += vz * step_size
                dist = distance(sun.x, sun.y, sun.z, x, y, z)
                if 0.99 < dist < 1.01 and -0.01 < z < 0.01:
                    return True

        elif abs(yy) > abs(xx) and abs(yy) > abs(zz):
                steps = int(abs(yy) / 0.00001)
                step_size = t / steps
                for _ in range(steps):
                    x += vx * step_size
                    y += vy * step_size
                    z += vz * step_size
                    dist = distance(sun.x, sun.y, sun.z, x, y, z)
                    if 0.99 < dist < 1.01 and -0.01 < z < 0.01:
                        return True

        else:
                steps = int(abs(zz) / 0.00001)
                step_size = t / steps
                for _ in range(steps):
                    x += vx * step_size
                    y += vy * step_size
                    z += vz * step_size
                    dist = distance(sun.x, sun.y, sun.z, x, y, z)
                    if 0.99 < dist < 1.01 and -0.01 < z < 0.01:
                        return True

    return False
```

This is also explained in Plot 3.4

Finally, to run the simulation it was used the function `Heartbeat`. If we only ask `REBOUND` to integrate a certain time, we can only see the beginning and end of the simulation. Nonetheless, using the function `Heartbeat` we can interact with the simulation in every step.

```
sim.heartbeat = heartbeat
sim.integrate(100000)
```

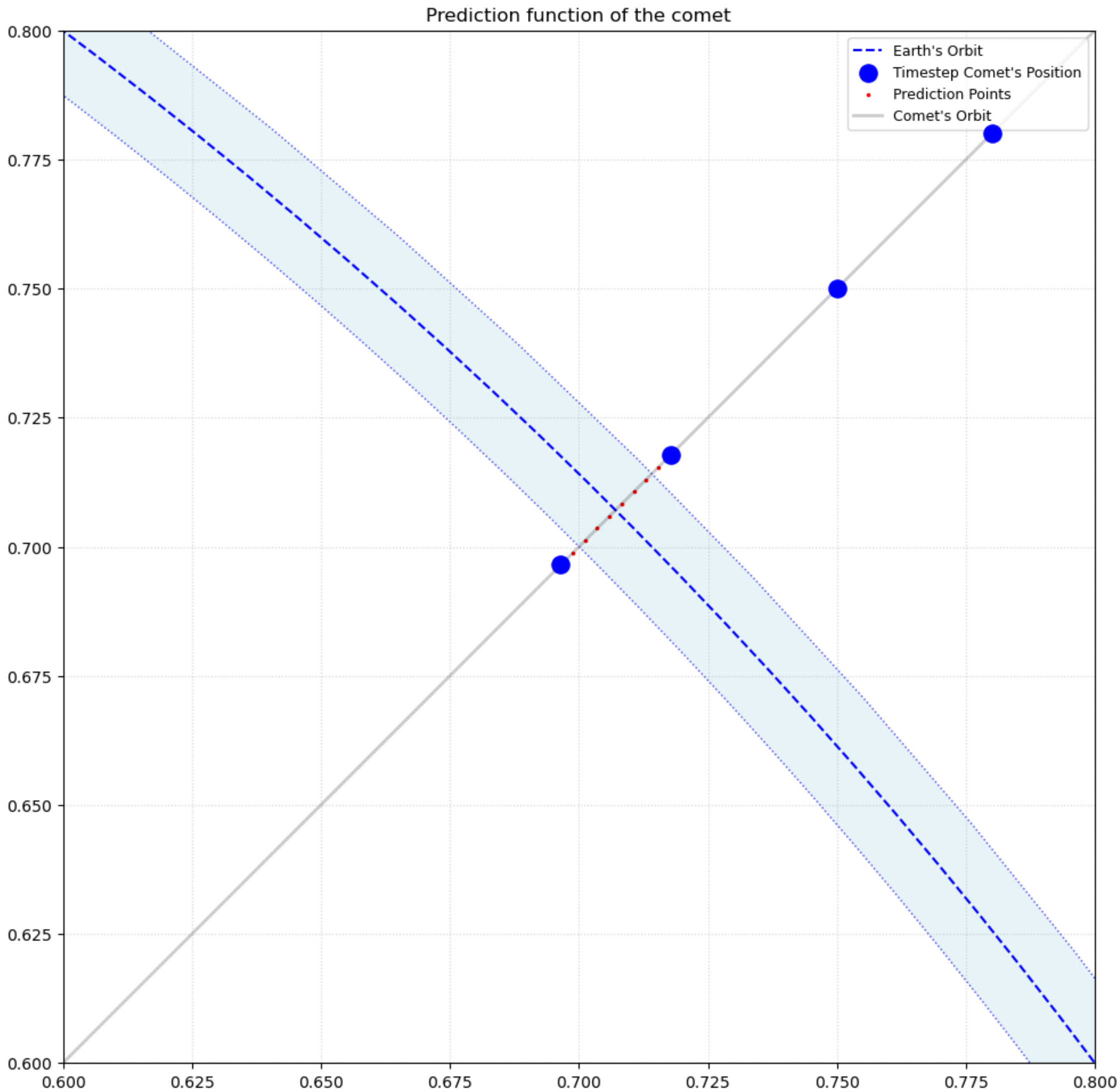

Figure 3.4: This plot displays an example of how the prediction function works, where the timestep of the comet jumps over the Hill zone, and the function creates points between those steps.

Testing the simulation, there were some problems. Every time a comet fell into the sun, the integrator switched to smaller and smaller time steps, until reaching a point when the simulation was stuck in the same time without advancing. It was necessary to predict when the comet was falling, and delete it.

Additionally, after running the simulation there were comets who disappeared. This happened because those comets reached higher velocities fast enough to escape the Solar System in a hyperbolic orbit ($e > 1$). For this case, our code detects the high speeds and deletes the comet to save resources.

There were added additional functions: To save all the information of the encounters and predictions through time, a function to save checkpoints of the simulation (to avoid losing the results in case of a blackout), and a function to send a message each 1.000 years to the state of the simulation.

Initially, this code was implemented in `Python` using `REBOUND` interface. However, when it was tried to simulate 1000 comets, the integration time was alarmingly low. It took 5 minutes approximately to run less than 2 years. At this rate, our simulation would have been running 200 days. Because of this, it was chosen to migrate to the native version of `REBOUND` in C, which was significantly faster. The complete simulation took approximately one week.

Chapter 4

Results

There were run 4 simulations in total to compare results:

- A simulation with NGF and with solar system planets
- A simulation with NGF and without planets
- A simulation without NGF and with solar system planets
- A simulation without NGF and without planets

As defined in Section 3, an encounter corresponds to the comet crossing the Hill's ring ($0.99 < r < 1.01$ AU), meaning may have entered Earth's gravitational sphere of influence, not a direct physical collision. The results are in Plot 4.1. Here we can see the Cumulative Frequency of encounters within the Hill's ring over time. The number of encounters is ordered from highest to lowest, mirroring the order of the simulations, with the colors blue, orange, green, and red. In all simulations, there is an exponential increase in encounters, which subsequently stabilizes. This corresponds to comets whose orbits were already intertwined with Earth's orbit from the time comets were defined, without the need for interaction with the NGF or planets. This explains why the last simulation in red (without the NGF and without planets) does not subsequently increase and remains constant over time. The comets maintain their initial positions unchanged, as there are no agents to alter them.

The green color then represents the simulation with planets and without NGF. The number of encounters increases steadily over time, without the effect of NGF. The properties of the comets most affected in this simulation will be evaluated later. However, we note that in this simulation, even without NGF, the number of encounters is almost 10 times greater than without planets.

In the orange and blue simulations, the number of encounters is approximately 30% and 60% higher than in the previous simulation respectively, where in both cases the NGFs are applied, and the greatest number of encounters occurs with the planets of the solar system.

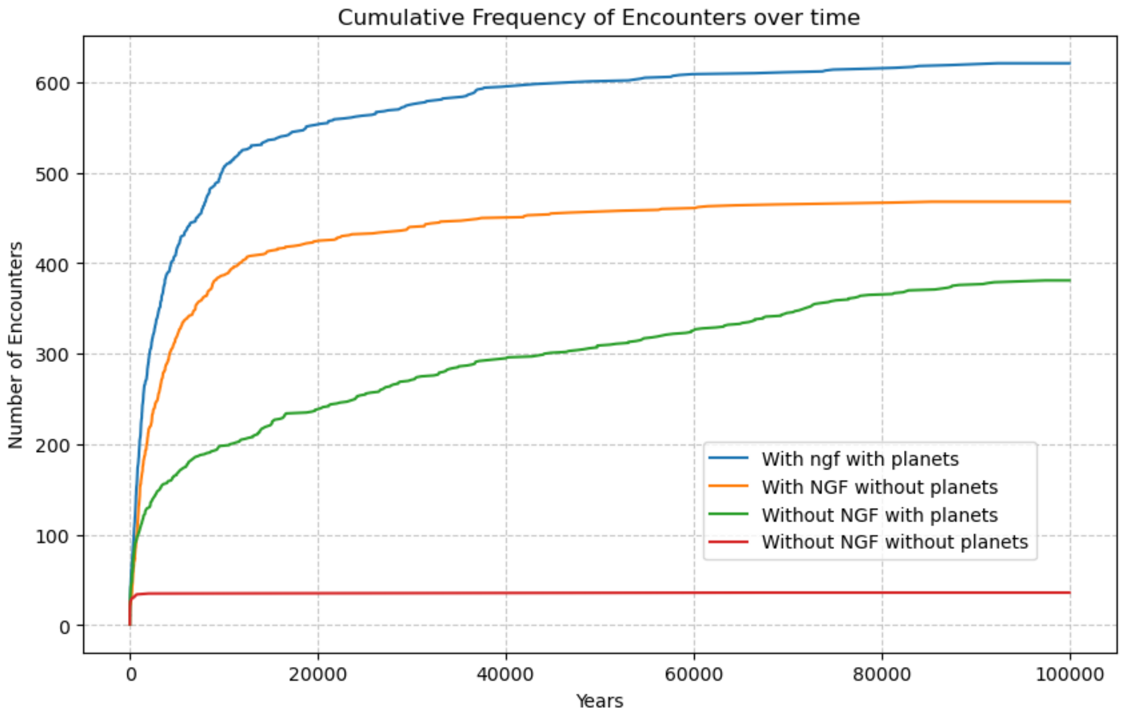

Figure 4.1: This plot displays the cumulative frequency of the Hill's ring encounters over time (until 100.000 years). They're displayed in order of colors as described in the list 4, with the colors blue, orange, green and red respectively. On the first quarter there is a noticeable increase on the encounters for the first three simulations, while the last red simulation (without NGF and without planets) doesn't increase.

In all simulations, there is a significant increase in the number of encounters in the early years, which gradually stabilizes over time, resulting in fewer encounters per year. This initial behavior occurs because some comet's orbits have initial positions close to Earth's orbit, where its initial positions are close to Hill's ring. Every small gravitational or non-gravitational interaction is enough to make them cross the encounter zone. Once the rate stabilizes, the number of encounters increases steadily over time, reflecting the long-term dynamical evolution of the cometary population. To better understand why some comets have encounters with Earth and others do not, we analyzed the orbital evolution of comets that did indeed encounter Earth. It is important to note that these comets represent a specific subpopulation: those that were already close to Earth's orbit or that managed to approach it in a relatively short time. Therefore, although they are not representative of the long-term evolution of the Solar System, they do allow us to identify the physical mechanisms that facilitate encounters. To distinguish between the effect of planets and that NGFs, we compared simulations with and without planets, keeping the NGF parameters constant (and vice versa). In this way, we can isolate the contribution of each mechanism.

Subsequently, an analysis of encounters is performed according to comet family, shown in the

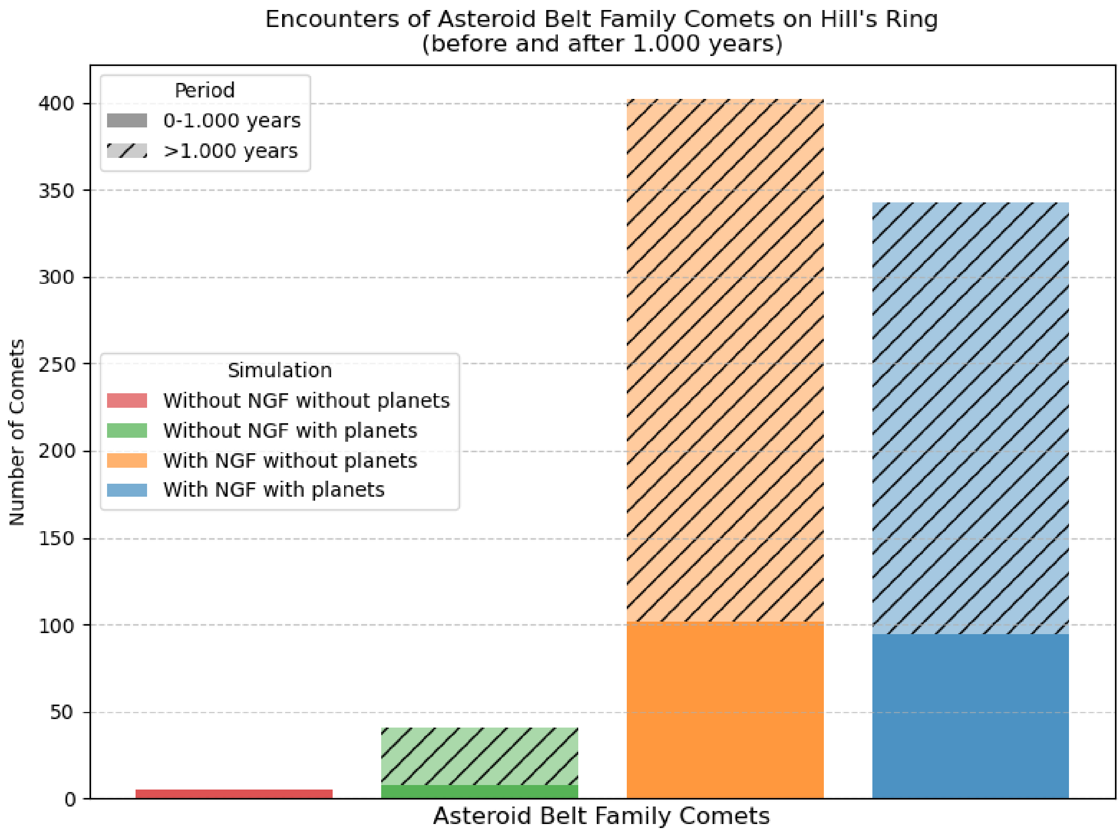

Figure 4.2: This graph is a histogram of the number of encounters over time for comets from the Asteroid Belt family, based on their final conditions. The colors are the same as in the previous graph for each simulation. The total height of each bar represents the total number of encounters over time, with the solid color area representing the first 1.000 years and the dashed area representing subsequent years. It is evident that near-Earthquakes are necessary for encounters to occur.

following three graphs. Plot 4.2 represents a histogram of the number of encounters over 100.000 years of comets from the Asteroid Belt family, according to their final conditions (at the time of the encounter). The colors for each simulation are maintained according to the previous graph and are ordered inversely to the list of comet items, from fewest to most encounters, from left to right. It is evident that without the NGF, the number of encounters is minimal compared to with the NGF, regardless of whether planets are present. This makes sense since they are not located in the region of Jupiter's orbit. However, with NGF and without planets, there are more encounters (orange) than with NGF and with planets (blue), suggesting that planetary perturbations may slightly reduce the effectiveness of NGF in bringing comets into the Hill's ring. This could be because planetary scattering removes some comets from the near-Earth region before NGF can act. However, the difference is not highly statistically significant, and should be interpreted with caution. Larger simulations would be needed to confirm this trend.

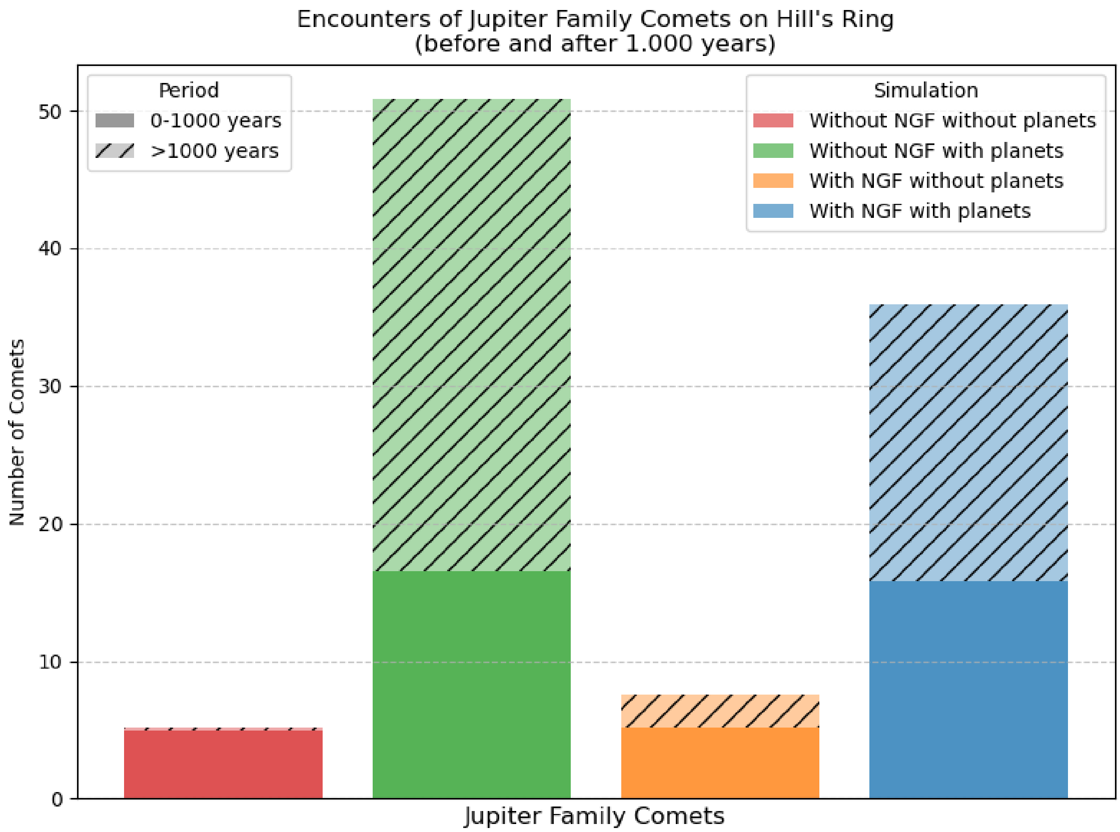

Figure 4.3: This graph is a histogram of the number of encounters over time for comets from the Jupiter family, based on their final conditions. The colors are the same as in the previous graph for each simulation. The total height of each bar represents the total number of encounters over time, with the solid color area representing the first 1,000 years and the dashed area representing subsequent years. It is noticeable that the effect of Jupiter is more impactful than NGF.

Plot 4.3 represents a histogram of the number of encounters over 100.000 years of comets from the Jupiter family, according to their final conditions (at the time of the encounter). The colors for each simulation are maintained according to the previous graph. Here, most of the encounters occur without NGF and with planets (green), followed by with NGF and with planets (blue). Here, the effect of the planets, primarily Jupiter, has more impact in increasing the encounters than the NGF, which it makes sense since NGF have less effect in further distances.

Plot 4.3 represents a histogram of the number of encounters over 100,000 years of comets from the Oort family, according to their final conditions (at the time of the encounter). The colors for each simulation are maintained according to the previous graph. Similarly to the last plot, most encounters occur in the simulation without NGF and with planets (green), followed by the simulation with NGF and with planets (blue). This indicates that at greater distances from the Sun, the effect of planetary perturbations, particularly from Jupiter, dominates over non-gravitational forces. In these outer regions, NGF are less effective because sublimation is weaker,

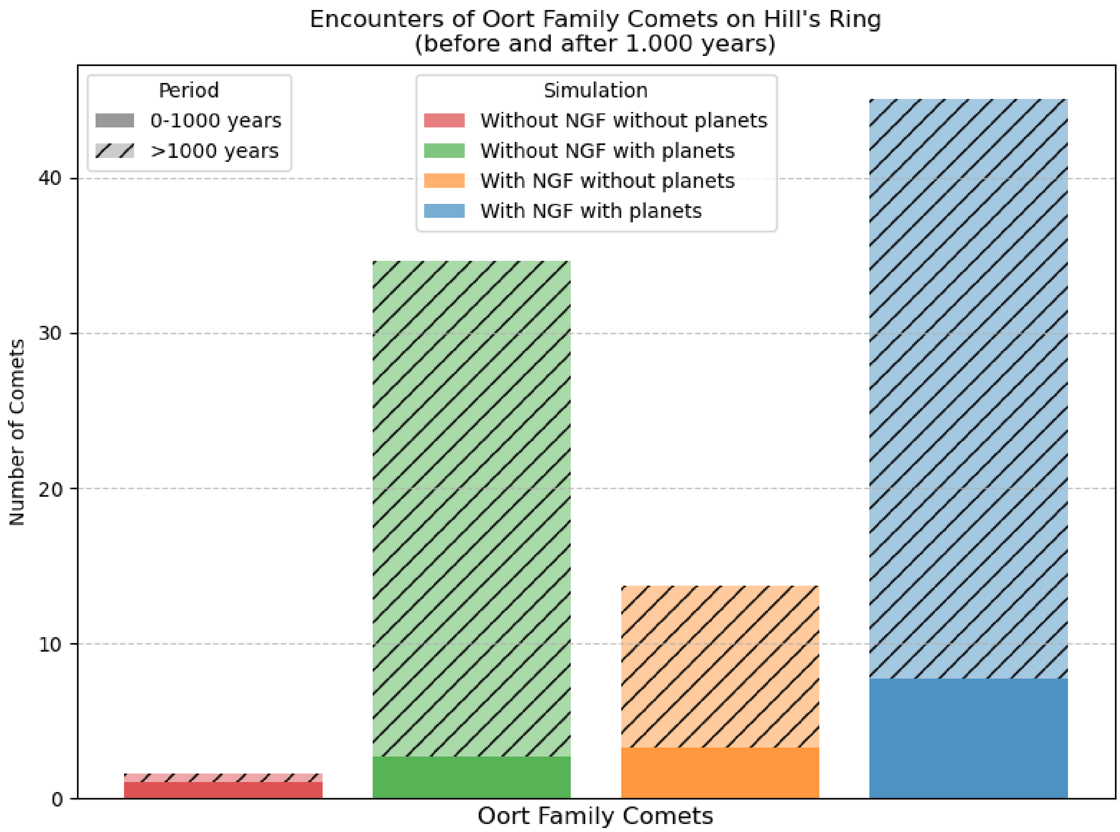

Figure 4.4: This graph is a histogram of the number of encounters over time for comets from the Oort family, based on their final conditions. The colors are the same as in the previous graph for each simulation. The total height of each bar represents the total number of encounters over time, with the solid color area representing the first 1.000 years and the dashed area representing subsequent years. It is noticeable that the effect of Jupiter is more impactful than NGF.

and the comets' orbital evolution is primarily driven by gravitational interactions with the giant planets.

The summary of the last three plots are together in Plot 4.5. Most encounters are with comets from the asteroid belt, which are also the closest to Earth's orbit. In this simulation, the greatest number of encounters occur with NGFs, both with and without planets (orange and blue), while in the Jupiter and Oort family, the greatest number of encounters occur with planets. This is more significant than with NGFs because planets have less of an effect at greater distances. In most cases, there are more encounters after the first thousand years than before, demonstrating that encounters occur over time as the orbital properties of comets change.

The Plot 4.6 has the same information of the histograms as Plot 4.5, but with the percentage of encounters by family. It is considered the amount of initial comets with their initial properties, and the final properties of the comets in their encounters. The percentage of comet encounters on the Asteroid Belt family exceeds 100%, which is interpreted as comets from other families turning

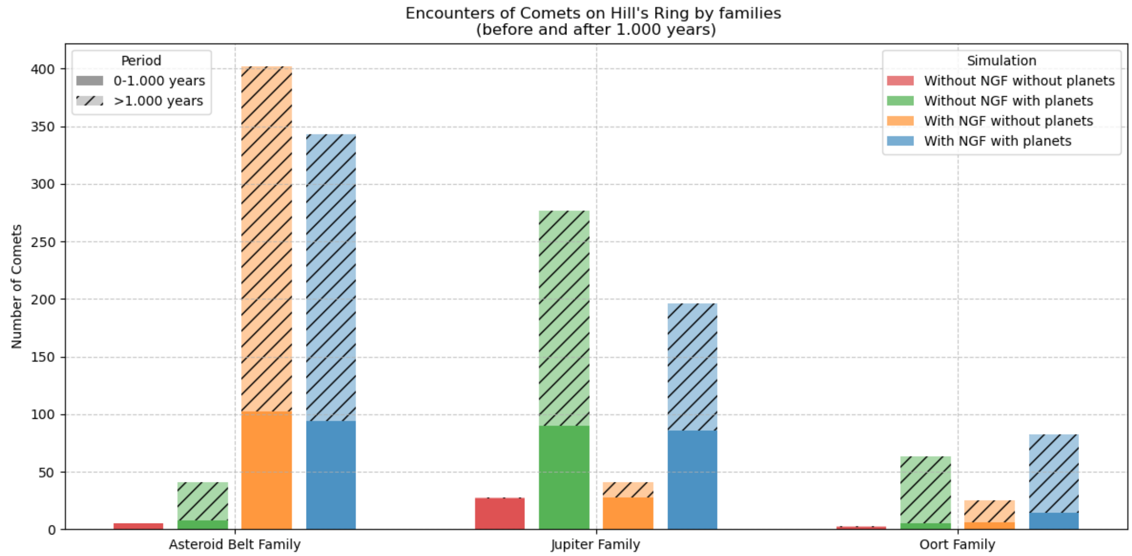

Figure 4.5: This graph is a histogram of the number of encounters over time for comets separated by family, based on their final conditions. The colors are the same as in the previous graph for each simulation. The total height of each bar represents the total number of encounters over time, with the solid color area representing the first 1,000 years and the dashed area representing subsequent years. Most of the impacts occur on the Asteroid Belt family.

into Asteroid Belt family. This is going to be reviewed in detail in the next plots.

To understand how comet orbits change over time due to the NGF, the same simulation was run without planets for a thousand years, recording the changes over time. The results are presented in the following graphs, separated by families. Changes in the Asteroid Belt family are shown in Figure 4.7, where the former represents the change in the semi-major axis and the latter the change in eccentricity. Each colored line represents a comet, with the star symbol indicating the moment the comet encountered the Hill ring. Almost all comets show a decrease in both the semi-major axis and eccentricity, resulting in a more circular orbit closer to the Sun. The average semi-major axis is approximately 1.4 AU. The only exception is a comet whose eccentricity increased (light blue).

The change in the Tisserand parameter T_J over time was calculated until each comet encountered the Hill ring, represented by the star in Plot 4.8. Most comets show a progressive increase in the Tisserand parameter T_J over time, which also indicates that their orbits become closer to the Sun and more circular. The only exception is the comet itself (shown in light blue), whose parameter is approaching the Jupiter family.

The evolution of the parameters of the Jupiter family comets are displayed in Figure 4.9, where the upper plot is the change of the major semi axis and the plot below is the change of the eccentricity. Most of the comets decrease their major semi axis, except a few that increase it. The mean major semi axis at the encounter moment is 2.84 AU. Most of the comets decrease their

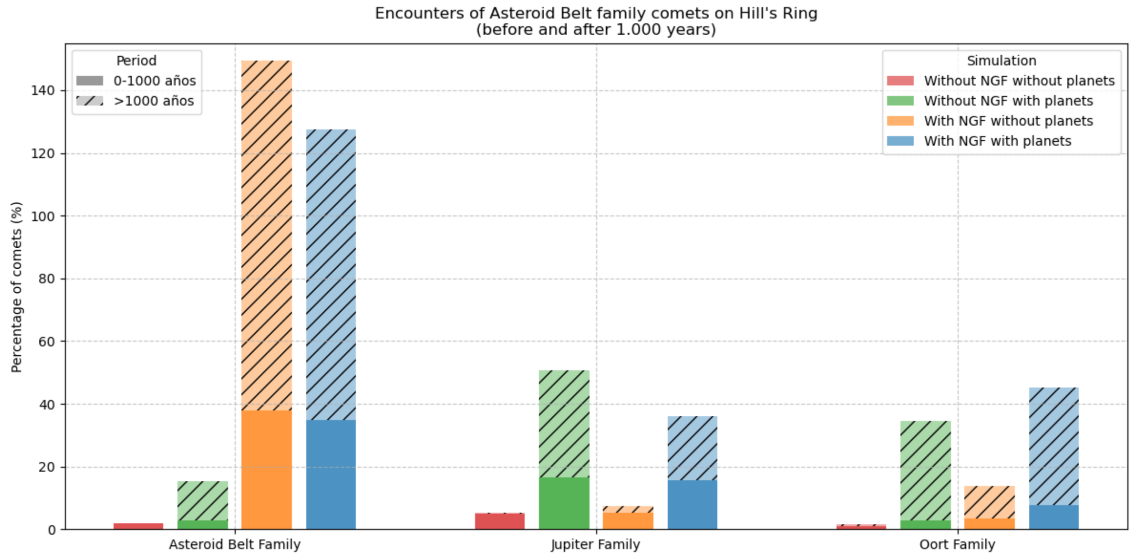

Figure 4.6: This graph is a histogram of the percentage of encounters over time for comets separated by family, based on their final conditions of the encountered comets and the comets initial amount. The colors are the same as in the previous graph for each simulation. The total height of each bar represents the total number of encounters over time, with the solid color area representing the first 1,000 years and the dashed area representing subsequent years. The percentage of encounters of the Asteroid Belt Family exceed 100%, which can only be explained by comets from other families turning into Asteroid Belt family comets.

eccentricity, forming more circular orbits, while the ones with initial eccentricity over 0.8 increase it.

The change in the Tisserand parameter T_J over time was calculated until each comet encountered the Hill ring, represented by the star in Plot 4.10. The parameter range for a Jupiter family comet is $T_J = [2, 3]$, where the comets start. After time, only a few of them continue inside that range. Some of them get lower, turning into Oort family comets (with wider orbits and more eccentric). Most of the comets increase their T_J exponentially, turning into Asteroid Belt family comets (smaller orbits and more circular).

The evolution of the parameters of the Oort family comets are displayed in Figure 4.11, where the upper plot is the change of the major semi axis and the plot below is the change of the eccentricity. In this period range there's only 5 encounters. The first one occurs at 0.20 years, where there isn't enough time for NGF to have effect. The second encounter occurs at 312.67 years (comet number 56), where the eccentricity barely changes, but the major semi axis increases in a very short period of time. The other 3 encounters happen to have similar situations, where all of their major semi axis and eccentricity decreases.

The change in the Tisserand parameter T_J over time was calculated until each comet encountered the Hill ring, represented by the star in Plot 4.12. The first two comets mentioned previously

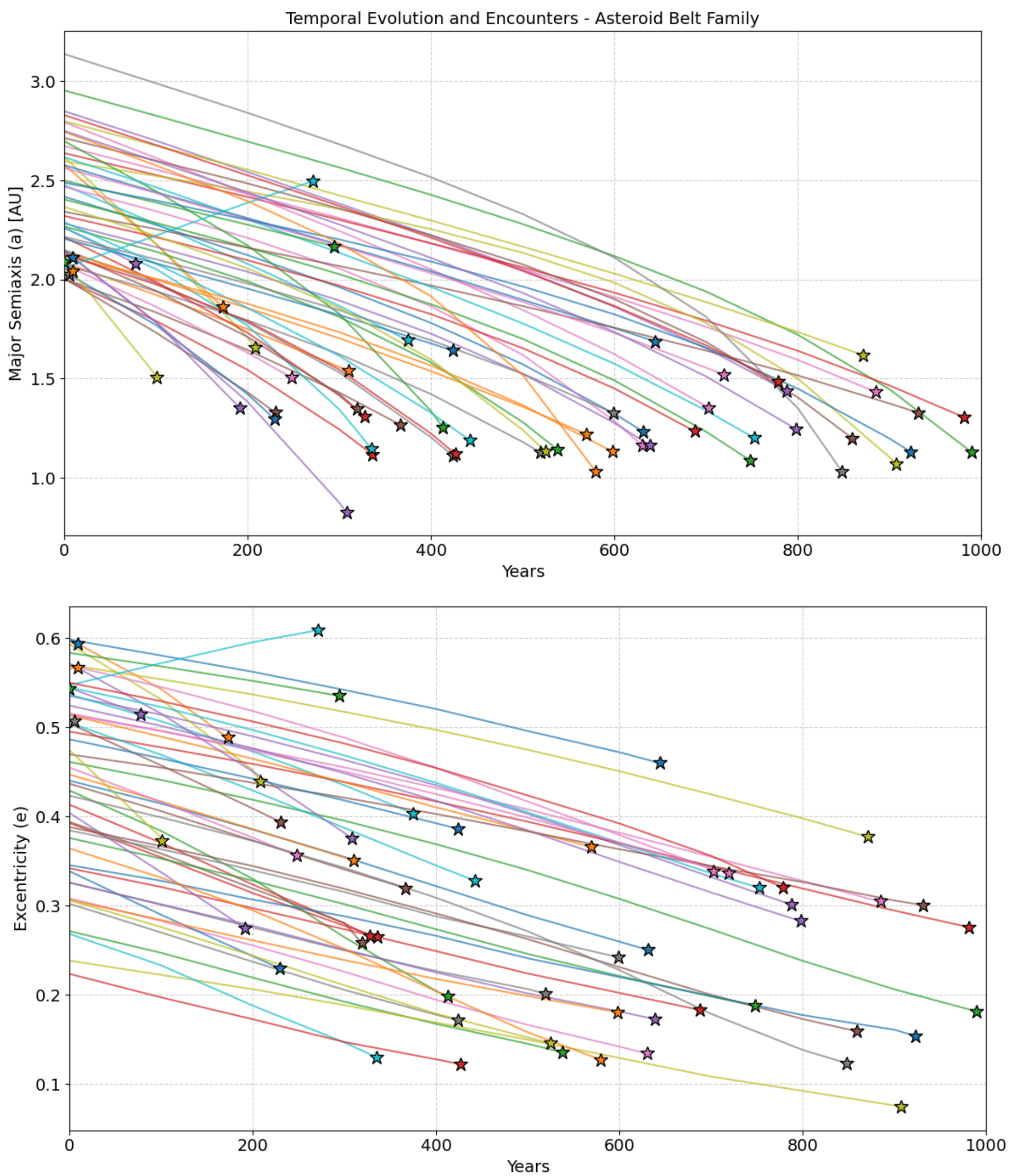

Figure 4.7: These plots represent the evolution of comets from the Asteroid Belt family over 1,000 years and the evolution of their orbital parameters over time until an encounter with the Hill ring (symbolized by the star in the graph). The upper plot shows the change in the semi-major axis, and the lower plot shows the variation in eccentricity. Most comets exhibit a decrease in the size of their semi-major axis and eccentricity, making their orbits more circular and closer to the Sun.

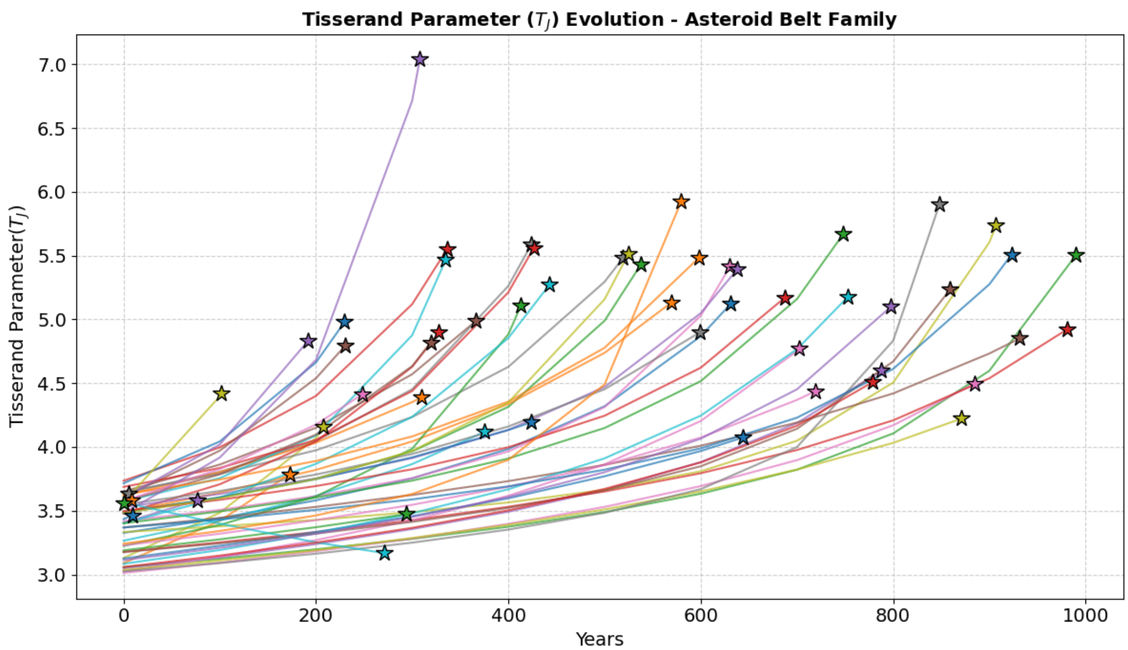

Figure 4.8: This plot represent the evolution of the Tisserand Parameter T_J of comets from the Asteroid Belt family over 1000 years or until an encounter with the Hill ring (symbolized by the star in the plot). In most of the comets the Tisserand Parameter T_J increases, representing their orbits get smaller and more circular.

maintained their family without variation. The other three comets increase their T_J exponentially, getting into the asteroid belt family, with smaller orbits and lower eccentricity.

This difference recalls mainly on the A_2 parameter from the NGF. When this parameter is positive, represents a **prograde rotation**. The NGF act in the same direction of the comet's movement, accelerating them and increasing their orbit's size. Nonetheless, when this parameter is negative, represents a **retrograde rotation**. Here the comet is rotating in the opposite direction of the movement, where the NGF act against their movement and work as a dynamic break. This way the comet expels gas towards the direction of its orbital motion, while its orbit's size and eccentricity decreases. This movement is represented by Figure 4.13. This can be seen in Plots 4.14, where they represent the families of the Asteroid Belt, Jupiter and Oort.

The same Tisserand Parameter T_J is plotted, with a colored bar representing their A_2 parameter using red for positive values and blue for negative ones. We notice most of the comets that advance to the same direction, to a bigger T_J, have a negative A_2 (blue). Similarly, those comets we mentioned that followed an opposite direction and lower their T_J have a positive A_2.

Ultimately, the parameter A_2 is the most important for increasing the number of comet encounters with Earth. Almost all encounters occur with a negative A_2, when comets decrease the size of their orbits to approach the size of Earth's orbit, thus decreasing their eccentricity. This

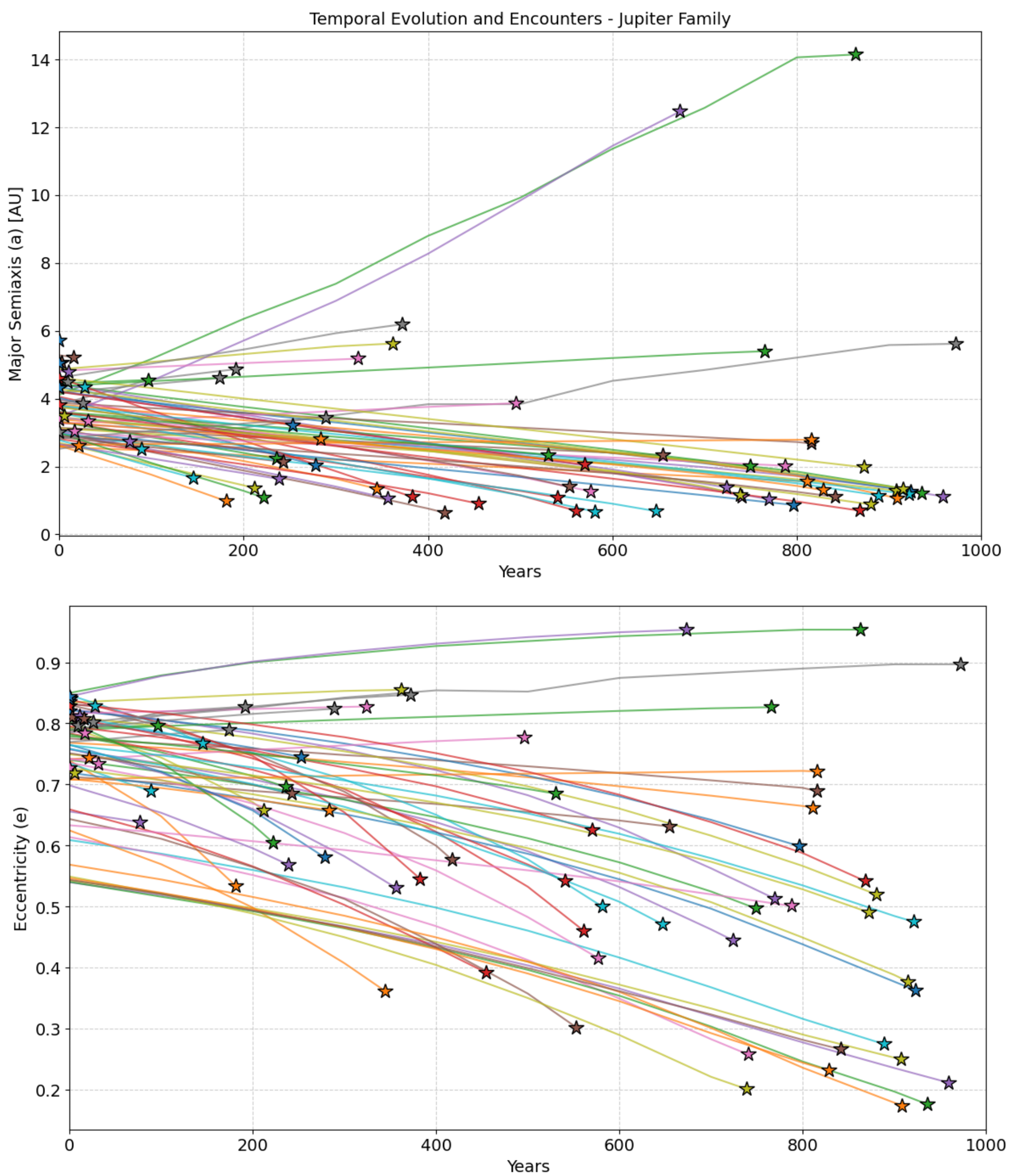

Figure 4.9: These plots represent the evolution of comets from the Jupiter family over 1,000 years and the evolution of their orbital parameters over time until an encounter with the Hill ring (symbolized by the star in the plot). The upper plot shows the change in the semi-major axis, and the lower plot shows the variation in eccentricity. Most comets exhibit a decrease in the size of their semi-major axis and eccentricity, making their orbits more circular and closer to the Sun.

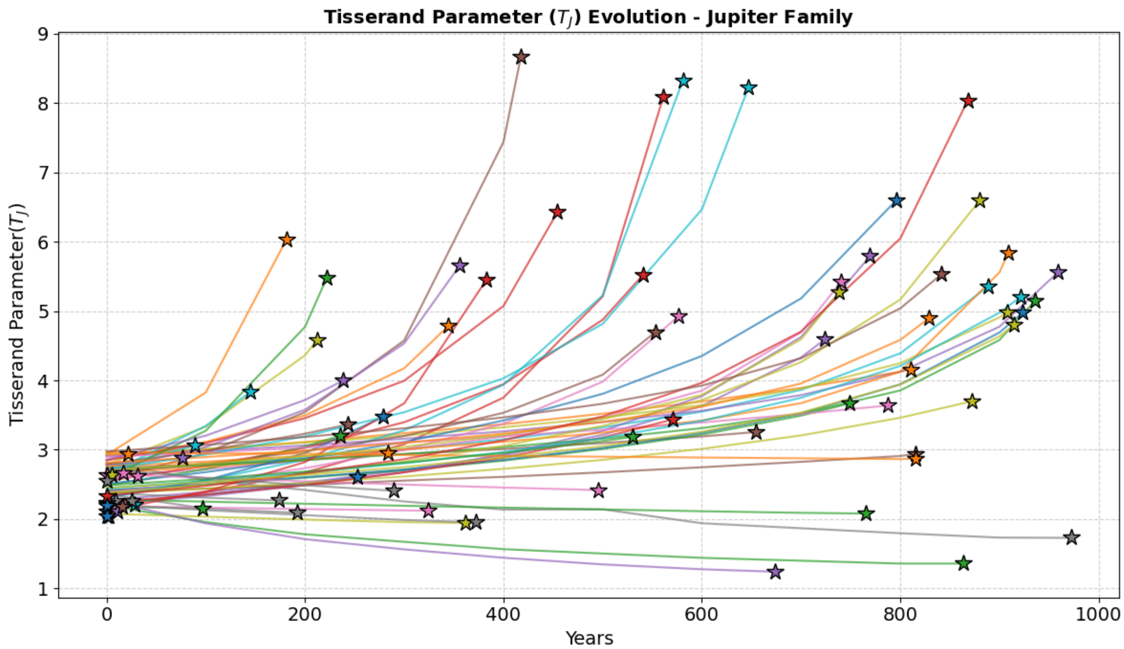

Figure 4.10: This plot represent the evolution of the Tisserand Parameter T_J of comets from the Jupiter family over 1000 years or until an encounter with the Hill ring (symbolized by the star in the plot). In most of the comets the Tisserand Parameter T_J increases, representing their orbits get smaller and more circular.

also causes the comets' speed to decrease, favoring an encounter. When the comet catalog was created, the probability of A_2 being positive was 50%. Since most encounters have a negative A_2, it demonstrates that it is a crucial condition for encounters to occur. However, there are exceptions where A_2 is positive, as the comet accelerates, increasing the size of its orbit and its eccentricity, ultimately resulting in an encounter (such as comet 56).

4.0.1 Limitations

For this simulations it was considered only the non-gravitational effects by Marsden et al.in 1973, which is the most standard and general model. Nevertheless, it has limitations and it can display differences in real comets, with the models described by Królikowska 2004.

First, there are differences with the long period comets. Marsden comet fits g(r) for the sublimation rate of water snow (H_2O), however, comets from the Oort cloud posses Carbon Monoxide (CO) ice or Nitrogen (N_2) ice, which can sublimate at longer distances than water. In our model, the contribution of NGF becomes negligible at distances smaller than 8 AU, so our code does not compute them outside this region. For other components, further distances continue to be relevant.

Additionally, there can be chances where the function computes unreal values. For long period comets, the function g(r) sometimes calculates radial acceleration (A_1) unacceptable big and phys-

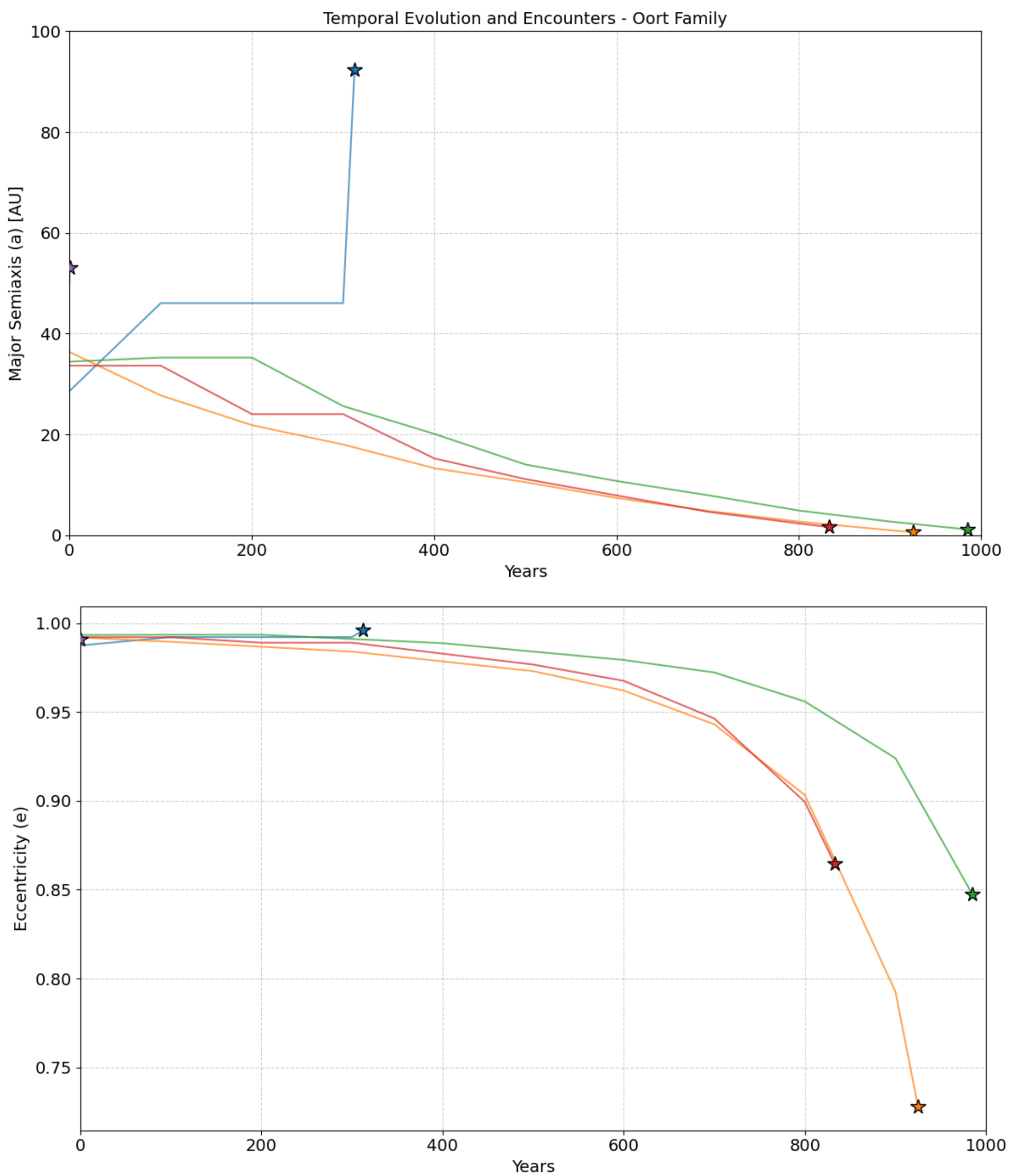

Figure 4.11: These plots represent the evolution of comets from the Oort family over 1000 years and the evolution of their orbital parameters over time until an encounter with the Hill ring (symbolized by the star in the plot). The upper plot shows the change in the semi-major axis, and the lower plot shows the variation in eccentricity. Their major semi axis is different, but their eccentricity lowers drastically.

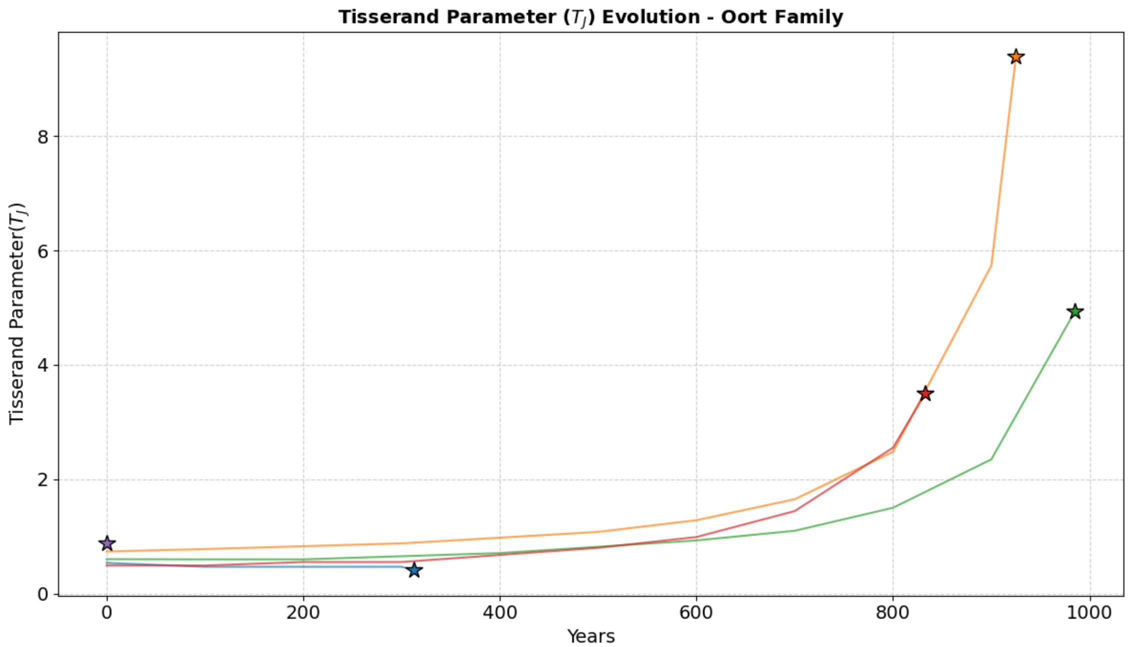

Figure 4.12: This plot represent the evolution of the Tisserand Parameter T_J of comets from the Oort family over 1000 years or until an encounter with the Hill ring (symbolized by the star in the plot). There are three comets where the orbit becomes smaller asteroid-belt like, while the other two remain.

ically not realistic. This occurs because Marsden et al. 1973 model was designed for short period comets (like 2P/Encke) that already lost their outlet ice layers and their A_1 parameter its smaller. For long period comets, that still haven't lost their ice shells, will have bigger A_1. Furthermore, comets like C/1998 P1 or C/1993 A1 display orbit variations because of CO expulsion in distances where the parameter A_1 would have a minimum value. Because of this their A_1 parameter would be "inflated" to bigger values to make the orbits fit Królikowska 2004.

On the contrary of the model we used for A_3, further studies (specially for long period comets) have proved that their A_3 is present in most of the comets, and sometimes its value is 5 times bigger than A_2 Królikowska 2004. This consideration is crucial for subsequent simulations.

The Marsden model (Marsden et al. 1973) assumes that non-gravitational forces are symmetric about perihelion. However, in 1989, Yeomans and Chodas developed the time-shift parameter (τ), which allows for the correction of some problematic orbits, such as that of comet C/1959 Y1 Burnham, by introducing a time-asymmetry. This parameter considers that out gassing can occur before or after perihelion due to the thermal inertia of the nucleus. Although this time-asymmetry has a different physical effect than the normal component A_3, the A_3 parameter has been used in some studies to model equivalent effects (Yeomans and Chodas 1989; Królikowska 2001).

There are more complex nucleus who need deeper components beyond A_1, A_2 and A_3, such as

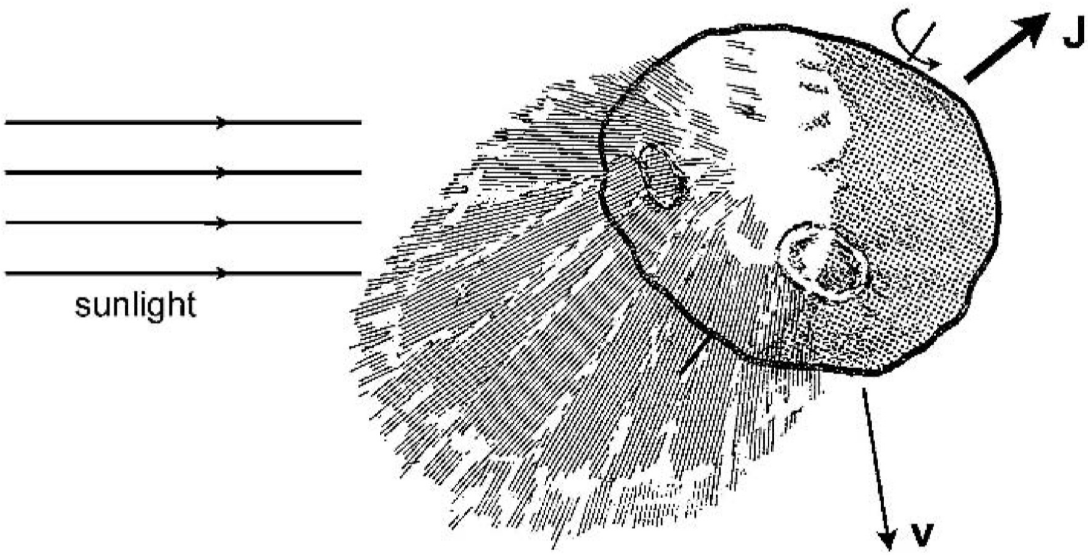

Figure 4.13: Representation of the origin of Non-Gravitational Forces (NGF) in a rotating cometary nucleus. Due to the thermal inertia of the surface material, the region of maximum temperature and out gassing does not coincide with the subsolar point (where the Sun is at its zenith), but rather shifts toward the "sunset" side of the nucleus, creating a thermal lag angle (λ). This jet of gas generates a net reaction force (J) in the opposite direction to the ejection. The component of this force projected in the direction of the orbital velocity (V) is defined as the transverse component, represented by the parameter A_2. In the case of prograde rotation (as illustrated), the force acts in the direction of motion, resulting in a positive A_2 value, which increases the orbital energy and period of the comet Fernández 2005

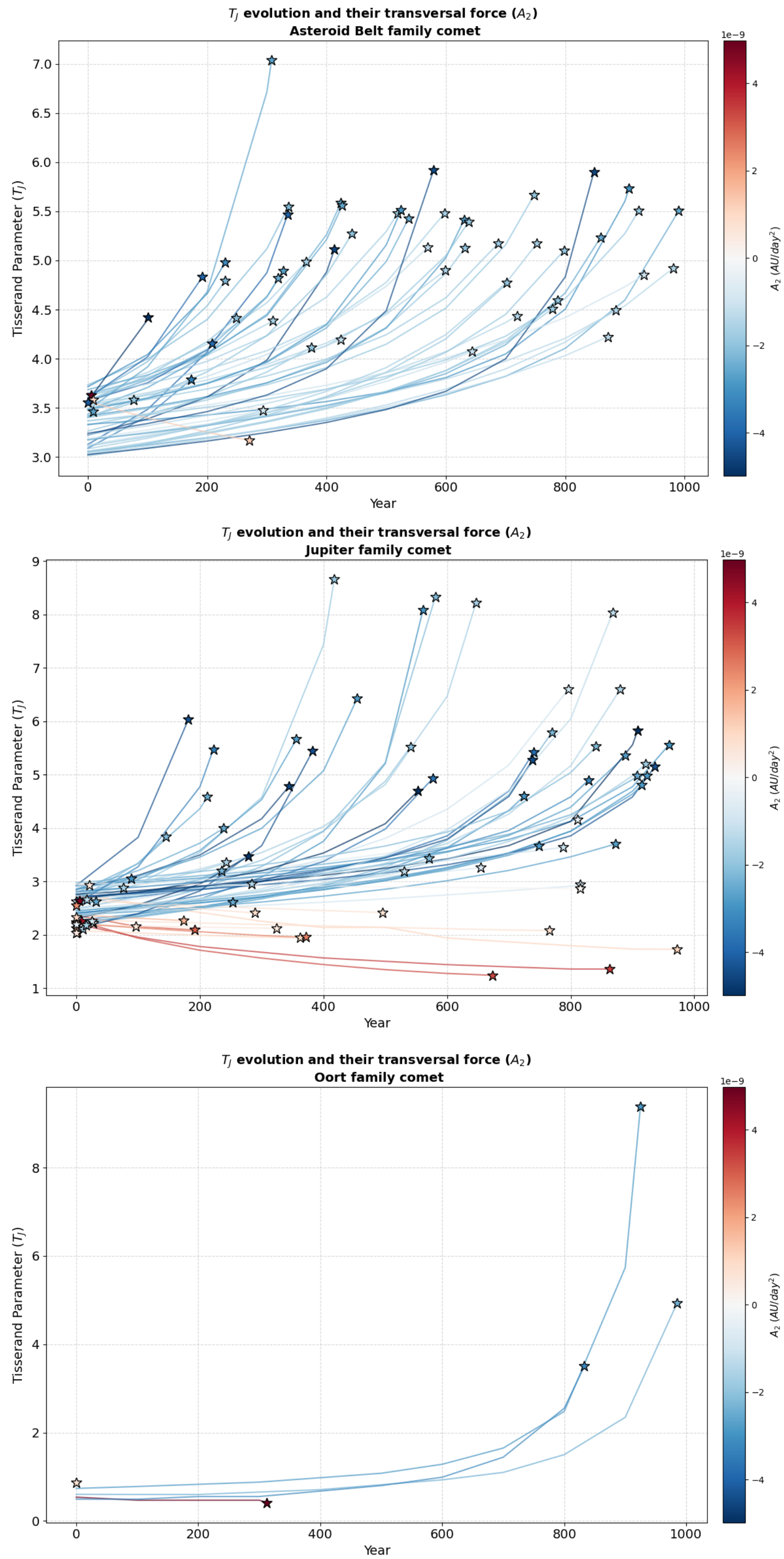

Figure 4.14: These plots represent the evolution of comets from each family (Asteroid Belt, Jupiter and Oort) over 1000 years and their A_2 parameter colored, which is the transversal force and direction of rotation. We can see that when A_2 is negative, the orbit slows down and becomes smaller, while when it's positive it accelerates and becomes bigger.

the delay angle (η) because of the degassing, or the models of forced precession from non-spherical nucleus generating torque.

Finally, there are models who are recommended depending of the scenario, such as the Sekanina Model (g_S), where the degassing is restricted to the subsolar point of the nucleus. There's the Yabushita Model ($f(r)$), that is specifically designed for the CO sublimation, which is preferred for newer comets. Even for more complex comets, such as Hale-Bopp and Hyakutake, there are personalized $g(r)$ functions adjusted to their components and scale distances (r_0), based on their photometric data.

The addition of these parameters and models could provide us more detailed and specific results considering a wider range of comets. Nevertheless, since our analysis was for the H_2O coming from comets, the models used where more certain.

Chapter 5

Conclusions

Four 100,000-year simulations were performed with 1,000 initial comets, combining the presence or absence of non-gravitational forces (NGFs) and planets in the Solar System. An encounter was defined as the crossing of Earth's Hill radius, considering that Earth could be at any point in its orbit (what we call the "Hill ring").

The results show that the simulation with NGFs and planets yielded more than 600 possible encounters (when the comet enters the Hill's ring zone). This was followed by a simulation with NGFs but no planets, resulting in approximately 480 encounters. Next, the simulation without NGFs but with planets reached almost 400 encounters, with a more gradual increase. Finally, the simulation without NGFs and without planets recorded only 36 encounters, all at the beginning of the simulation. Principally, a simulation without NGF when we add them, the possible encounters increase by 56%, that contrasts Morbidelli et al. 2000 low collision rate.

These results confirm that both non-gravitational forces and planetary perturbations contribute significantly to increasing the probability of comet encounters with Earth. However, the effect varies depending on the comet's dynamical family:

For asteroid belt comets ($T > 3$), NGFs are the dominant mechanism, as these comets are closer to the Sun, where sublimation is more effective.

For Jupiter-family comets ($2 < T < 3$), the effect of Jupiter is predominant, although NGFs also contribute.

For Oort cloud comets ($T < 2$), the effect of the planets is the only significant one, as NGFs are practically negligible at large distances from the Sun.

Our results demonstrate that the inclusion of non-gravitational forces (NGFs) increases the frequency of potential encounters with Earth by 56% compared to purely gravitational models. Analysis of orbital evolution shows that the transverse A_2 component of the NGFs, particularly when negative (retrograde), tends to reduce the semi-major axis and eccentricity of comets, bringing them closer to Earth's orbit and increasing their probability of encounter. This physical process acts as an injection engine toward the inner solar system, systematically raising the Tisserand parameter (T_J) as orbits become more circular and Earth-like (evolving toward the "Asteroid Belt Family"), making collisions statistically more probable.

Regarding the implications for the origin of water on our planet, these results suggest that non-gravitational forces may have played a fundamental role in delivering volatiles to early Earth by increasing the probability of comets with high sublimation rates encountering our planet. This dynamic compels a reconsideration of classical models such as that of Morbidelli et al. 2000, which limited the cometary contribution to a maximum of 10% based on a collision efficiency calculated using purely gravitational parameters. Finally, recent evidence from Lis et al. 2019 and Cordiner et al. 2025, which documents D/H ratios consistent with Earth's ocean water in hyperactive and Halley-type comets, reinforces the possibility that present-day water originates from comets whose impact probability is significantly higher than previously estimated due to the existence of NGFs.

References

Bottke, Jr., W. F., Vokrouhlický, D., Rubincam, D. P., and Broz, M. (2002). The Effect of Yarkovsky Thermal Forces on the Dynamical Evolution of Asteroids and Meteoroids. In Bottke, Jr., W. F., Cellino, A., Paolicchi, P., and Binzel, R. P., editors, *Asteroids III*, pages 395–408.

Chambers, J. and Wetherill, G. (1998). Making the terrestrial planets: N-body integrations of planetary embryos in three dimensions. *Icarus*, 136(2):304–327.

Chambers, J. E. (2012). Mercury: A software package for orbital dynamics. Astrophysics Source Code Library, record ascl:1201.008.

Cordiner, M. A., Gibb, E. L., Kisiel, Z., Roth, N. X., Biver, N., Bockelée-Morvan, D., Boissier, J., Bonev, B. P., Charnley, S. B., Coulson, I. M., Crovisier, J., Drozdovskaya, M. N., Furuya, K., Jin, M., Kuan, Y.-J., Lippi, M., Lis, D. C., Milam, S. N., Opitom, C., Qi, C., and Remijan, A. J. (2025). A d/h ratio consistent with earth's water in halley-type comet 12p from alma hdo mapping. *Nature Astronomy*, 9(10):1476–1485.

Delsemme, A. and Miller, D. C. (1971). Physico-chemical phenomena in comets—iii: the continuum of comet burnham (1960 ii). *Planetary and Space Science*, 19(10):1229–1257.

Dones, L., Weissman, P. R., Levison, H. F., and Duncan, M. J. (2004). Oort Cloud Formation and Dynamics. In Johnstone, D., Adams, F. C., Lin, D. N. C., Neufeeld, D. A., and Ostriker, E. C., editors, *Star Formation in the Interstellar Medium: In Honor of David Hollenbach*, volume 323 of *Astronomical Society of the Pacific Conference Series*, page 371.

Drake, M. J. (2005). Origin of water in the terrestrial planets. *Meteoritics & Planetary Science*, 40(4):519–527.

Eberhardt, P., Reber, M., Krankowsky, D., and Hodges, R. R. (1995). The D/H and Î8Ô/Î6Ô ratios in water from comet P/Halley. , 302:301.

Farinella, P. and Davis, D. R. (1992). Collision rates and impact velocities in the main asteroid belt. *Icarus*, 97(1):111–123.

Fernández, J. A. (1978). Mass removed by the outer planets in the early solar system. *Icarus*, 34(1):173–181.

Fernández, J. A. (2005). *Dynamics of LP Comets Entering the Inner Planetary Region*, pages 77–102. Springer Netherlands, Dordrecht.

Fernández, J. A. (1997). The formation of the oort cloud and the primitive galactic environment. *Icarus*, 129(1):106–119.

Franklin, F. and Lecar, M. (2000). On the transport of bodies within and from the asteroid belt. *Meteoritics & Planetary Science*, 35(2):331–340.

Gomes, R. (1997). Dynamical effects of planetary migration on the primordial asteroid belt. *Astronomical Journal v. 114, p. 396-401 (1997)*, 114:396–401.

Greenstreet, S., Ngo, H., and Gladman, B. (2012). The orbital distribution of near-earth objects inside earth's orbit. *Icarus*, 217(1):355–366.

Hahn, J. M. and Malhotra, R. (1999). Orbital evolution of planets embedded in a planetesimal disk. *The Astronomical Journal*, 117(6):3041–3053.

Królikowska, M. (2001). A study of the original orbits of "hyperbolic" comets. , 376:316–324.

Królikowska, M. (2004). Long-period comets with non-gravitational effects. *Astronomy & Astrophysics*, 427(3):1117–1126.

Levison, H. F. and Duncan, M. J. (1994). The long-term dynamical behavior of short-period comets. *Icarus*, 108(1):18–36.

Levison, H. F., Duncan, M. J., Zahnle, K., Holman, M., and Dones, L. (2000). Planetary impact rates from ecliptic comets. *Icarus*, 143(2):415–420.

Lis, D. C., Bockelée-Morvan, D., Güsten, R., Biver, N., Stutzki, J., Delorme, Y., Durán, C., Wiesemeyer, H., and Okada, Y. (2019). Terrestrial deuterium-to-hydrogen ratio in water in hyperactive comets. , 625:L5.

Lécuyer, C., Royer, A., Fourel, F., Seris, M., Simon, L., and Robert, F. (2017). D/h fractionation during the sublimation of water ice. *Icarus*, 285:1–7.

Marsden, B. G., Sekanina, Z., and Yeomans, D. (1973). Comets and nongravitational forces. v. *Astronomical Journal, Vol. 78, p. 211 (1973)*, 78:211.

Miozzi, F., Shahar, A., Young, E. D., Wang, J., Steele, A., Borensztajn, S., Vitale, S. M., Bullock, E. S., Wehr, N., and Badro, J. (2025). Experiments reveal extreme water generation during planet formation. *Nature*.

Morbidelli, A., Chambers, J., Lunine, J. I., Petit, J. M., Robert, F., Valsecchi, G. B., and Cyr, K. E. (2000). Source regions and timescales for the delivery of water to the earth. *Meteoritics & Planetary Science*, 35(6):1309–1320.

Nagasawa, M., Tanaka, H., and Ida, S. (2000). Orbital evolution of asteroids during depletion of the solar nebula. *The Astronomical Journal*, 119(3):1480–1497.

Oort, J. H. (1950). The structure of the cloud of comets surrounding the solar system and a hypothesis concerning its origin. *Bulletin of the Astronomical Institutes of the Netherlands, vol. 11, p. 91-110 (1950).*, 11:91–110.

Pfalzner, S., Davies, M. B., Gounelle, M., Johansen, A., Münker, C., Lacerda, P., Zwart, S. P., Testi, L., Trieloff, M., and Veras, D. (2015). The formation of the solar system. *Physica Scripta*, 90(6):068001.

Pollack, J. B., Hubickyj, O., Bodenheimer, P., Lissauer, J. J., Podolak, M., and Greenzweig, Y. (1996). Formation of the giant planets by concurrent accretion of solids and gas. *icarus*, 124(1):62–85.

Sekanina, Z. (1972). Rotation Effects in the Nongravitational Parameters of Comets. In Chebotarev, G. A., Kazimirchak-Polonskaia, E. I., and Marsden, B. G., editors, *The Motion, Evolution of Orbits, and Origin of Comets*, volume 45 of *IAU Symposium*, page 294.

Sekanina, Z. (1981). Rotation and Precession of Cometary Nuclei. *Annual Review of Earth and Planetary Sciences*, 9:113.

Sekanina, Z. (1988). Outgassing Asymmetry of Periodic Comet Encke. I. Apparitions 1924-1984. , 95:911.

Sekanina, Z. (2021). On the Detection and Distribution of Nongravitational Accelerations in the Motions of Long-Period Comets. *arXiv e-prints*, page arXiv:2109.11120.

Stimpfl, M., Lauretta, D., and Drake, M. (2004). Adsorption as a mechanism to deliver water to the earth. *Meteoritics and Planetary Science Supplement*, 39:5218.

Vokrouhlický, D., Bottke, W. F., Chesley, S. R., Scheeres, D. J., and Statler, T. S. (2015). *The Yarkovsky and YORP Effects*. University of Arizona Press.

Ward, W. R., Colombo, G., and Franklin, F. (1976). Secular resonance, solar spin down, and the orbit of mercury. *Icarus*, 28(4):441–452.

Whipple, F. L. (1950). A comet model. I. The acceleration of Comet Encke. , 111:375–394.

Yeomans, D. and Chodas, P. (1989). An asymmetric outgassing model for cometary nongravitational accelerations. *Astronomical Journal (ISSN 0004-6256), vol. 98, Sept. 1989, p. 1083-1093.*, 98:1083–1093.